Developmental and biophysical determinants of grass leaf size worldwide

Authors: *Alec S. Baird[1*], Samuel H. Taylor[2,3], Jessica Pasquet-Kok[1], Christine Vuong[1], Yu Zhang[1], Teera Watcharamongkol[3,4], Christine Scoffoni[1,5], Erika J. Edwards[6], Pascal-Antoine Christin[3], Colin P. Osborne[3], Lawren Sack[1*]*

Affiliations:

[1]Department of Ecology and Evolutionary Biology, University of California Los Angeles, 621 Charles E. Young Drive South, Los Angeles, CA 90095, USA.

[2]Lancaster Environment Centre, University of Lancaster, Lancaster LA1 4YW, UK.

[3]Department of Animal and Plant Sciences, University of Sheffield, Sheffield S10 2TN, UK.

[4]Faculty of Science and Technology, Kanchanaburi Rajabhat University, Muang District, Kanchanaburi, Thailand 7100.

[5]Department of Biological Sciences, California State University Los Angeles, 5151 State University Drive, Los Angeles, CA 90032, USA.

[6]Department of Ecology and Evolutionary Biology, Yale University, New Haven, CT 06520, USA.

*Correspondence to: alecsbaird@gmail.com and lawrensack@ucla.edu

Abstract

One of the most striking ecological trends is the association of small leaves with dry and cold climates, described 2400 years ago by Theophrastus, and recently recognized for eudicotyledonous plants at the global scale[1-3]. For eudicotyledons, this pattern is attributed to small leaves having a thinner boundary layer to avoid extreme leaf temperatures[4], and their developing vein traits that improve water transport under cold or dry climates[5,6]. Yet, the global distribution of leaf size and its mechanisms have not been tested in grasses, an extraordinarily diverse lineage, distinct in leaf morphology, which contributes 33% of terrestrial primary productivity, including the bulk of crop production[7]. Here we demonstrate that grasses have shorter and narrower leaves under colder and drier climates worldwide. We show that small grass leaves have thermal advantages and vein development that contrast with those of eudicotyledons, but that also explain the abundance of small leaves in cold and dry climates. The worldwide distribution of grass leaf size exemplifies how biophysical and developmental processes result in convergence across major lineages in adaptation to climate globally, and highlights the importance of leaf size and venation architecture for grass performance in past, present and future ecosystems.

The grasses (family Poaceae) originated at least 55 Mya[8] and include ~11,500 species in 750 genera[9], dominating up to 43% of the Earth's surface[7] (Fig. 1). Small leaves have been linked with arid climates in specific grass lineages and communities (Supplementary Table 1). A worldwide climatic association could importantly influence species' distributions, tolerance of climate change, and crop breeding. We tested relationships of leaf size with climate across 1752 grass species from 373 genera in a global database and for 27 diverse and globally distributed species in a common garden (Extended Data Fig. 1, Supplementary Table 2 and 3).

We also tested for an adaptive basis for the association of grass leaf size with climate (Fig. 1). Because smaller leaves couple more tightly with air temperature due to their thinner boundary layer, small-leafed eudicots avoid damage from night-time chilling and daytime overheating[4], and they may also achieve higher photosynthetic rate and water use efficiency and compensate for shorter growing periods[4,10-12]. We evaluated these potential advantages for small leafed grasses using energy balance modeling.

Smaller leaves may also develop vein traits that confer stress tolerance[5]. In typical eudicots, the large ("major") veins are patterned before the bulk of leaf expansion[5], and leaves that expand less have narrower major veins and xylem conduits, and major veins more closely spaced, resulting in a higher major vein length per leaf area (major VLA)[5,6]. Across eudicots, major vein traits scale allometrically with mature leaf size:

$$\text{Trait} = a \times \text{leaf area}^{b} \quad (1)$$

where a is a scaling coefficient and b the scaling exponent[13]. These major vein traits in small eudicot leaves can provide greater water transport and lower vulnerability to freezing and dehydration[6] (Fig. 1a, Supplementary Table 4). Yet grass leaves are highly distinct, with parallel longitudinal veins connected by transverse veins[14]. To determine vein scaling, and its adaptive consequences for small grass leaves, we synthesized a model of C_3 and C_4 grass leaf development (Box 1, Table 1). For 27 grass species in a common garden, we compared the predicted scaling relationships against null expectations from geometric scaling[5,13] (Extended Data Fig. 1, Supplementary Table 3). We tested whether developmental scaling would confer small leaves with potential climatic advantages.

Box 1. *Synthetic model of grass leaf vein development based on published data for 20 species (Supplementary Tables 5-6), conferring small leaves with traits advantageous under cold and dry climates*

Grass leaf development includes five phases based on developmental zones:

Phase P (formation and expansion of the primordium, P): "Founder cells" in the periphery of the shoot apical meristem generate the leaf primordium. Cell divisions drive growth of a hood-like structure, in which the central 1° vein (midvein) and the large 2° veins are initiated early and extend acropetally, enabling their prolonged diameter growth (Box 1 Fig. 1a, c, e). Henceforth, discrete spatial growth zones develop at the leaf base and drive leaf expansion laterally and longitudinally.

Phase D (formation of the cell division zone, DZ): The basal cell division zone (DZ) expands slightly, driving minimal growth (Box 1 Fig. 1a, b). The 1° and 2° vein orders (major veins) complete their patterning basipetally along the leaf blade and increase in diameter (Box 1 Fig. 1c, e). Meanwhile, beginning at the lamina tip, C_3 species form a single order of small longitudinal minor veins, i.e., 3° veins, as do most C_4 species, i.e., $C_{4\text{-}3L}$ species. Some C_4 species of the subfamily Panicoideae additionally form smaller 4° veins, i.e., $C_{4\text{-}4L}$ species[15] (Box 1 Fig. 1c).

Phase D-E (DZ, and formation of the expansion zone, EZ): Cells from the DZ transition to a distinct, distal expansion zone (EZ). In the EZ, cell expansion in width and length spaces apart the 1° and 2° veins, resulting in the declines in their vein length per leaf area (Box 1 Fig. 1a, b, d). Additional 3° veins (and in some species, 4° veins) continue to initiate at the leaf tip between major vein orders and extend basipetally (Box 1 Fig. 1c-e). The transverse 5° veins form last, connecting the longitudinal veins.

Phase D-E-M (DZ, EZ and the maturation zone, MZ): Cells from the EZ mature distally, generating the maturation zone (MZ), which increases in size as cells file through the developmental zones (Box 1 Fig. 1a). The venation xylem, phloem and bundle sheath mature.

Phase M (all leaf is MZ): Leaf development is complete with all cells differentiated and expanded (Box 1 Fig. 1a-b).

Given that this developmental model is conserved across grass species, scaling predictions can be derived for species varying in leaf size (Supplementary Table 6). Some of these scaling relationships arise intrinsically from the sequence of development. Thus, major vein length per area (VLA) would be lower in wider leaves, as their major veins are spaced further apart. The 1° VLA declines geometrically as the inverse of leaf width, whereas the 2° VLA would decline less steeply than geometrically, as the formation of more 2° veins would partially counteract their greater spacing. Other scaling trends are not intrinsic, but "enabled" by the developmental program[15]. The diameters of 1° and 2° veins are expected to scale positively with leaf length and area, because a greater leaf length expansion rate or duration enables greater vein diameter growth. Similarly, a positive scaling of 1° and 2° vein xylem conduit diameters with vein diameter is enabled by the greater vein expansion in larger leaves.

Minor veins differ from major veins in their predicted scaling with leaf size across species. As minor veins are initiated at the developing leaf tip, greater length expansion provides more space and time for initiating additional minor veins, and thus minor VLA would scale positively with final leaf length. However, as minor veins are initiated later during leaf width expansion, and their diameter growth and spacing is more limited, their vein traits would be independent of final width. The positive scaling of minor VLA with leaf length and its decoupling from leaf width would result in a weak positive scaling of minor VLA with leaf area. Total VLA, i.e., summing major and minor veins, would be decoupled from leaf area, due to the negative scaling of major VLA with leaf width and the positive scaling of minor VLA with leaf length. Additional scaling predictions arise from the scaling of vein diameters and lengths with leaf size (Supplementary Table 6). Like major vein diameters, vein surface and projected areas and volumes per leaf area (VSA, VPA and VVA, respectively) would scale positively with leaf length, and, like major VLA, negatively with leaf width. These counteracting trends lead to predictions that VSA, VPA and VVA are decoupled from leaf area.

The developmental model predicts that grass species with smaller leaf dimensions would develop vein traits conferring stress tolerance, including narrower major veins and higher major VLA, VSA, VPA and VVA, which contribute to water transport efficiency and lower vulnerability to cold and drought[5,6] (Fig. 1a, Supplementary Table 4). Yet, large grass leaves can attain high minor and total VLA, VSA, VPA and VVA, independently of leaf size, enabling high transport efficiency to compete in sunny, moist climates.

C_3 and C_4 species were predicted to converge in their vein scaling. C_4 grasses have higher total VLA, providing a large vein bundle sheath compartment for concentrating CO_2 to enable high rates of photosynthetic assimilation[15-17]. We hypothesized the high total VLA of C_4 grasses arises from minor VLA, and therefore independently of leaf area.

Relationship of leaf size with climate

Globally, grasses vary by more than 625-fold, 275-fold, and 160,000-fold in leaf length, width and area respectively[8,18] and smaller leaves are associated with cooler and drier climates (Fig. 1b, 1c; Supplementary Tables 1-2, 7). Across species, leaf length, width and area were inter-related, and all were positively correlated with mean annual temperature (MAT), mean annual precipitation (MAP), and aridity index (AI) (for leaf area, $r = 0.24$-0.31, $P < 0.001$; phylogenetic $r = 0.08$-0.17, $P < 0.001$; Fig. 1c, Extended Data Fig. 2, Supplementary Table 7). Similar relationships were found with growing season temperature and precipitation (GST and GSP, respectively) and growing season length (Supplementary Table 7). The climatic associations of smaller leaves were independent of plant stature, and statistically similar for C_3 and C_4 species (Supplementary Tables 7-8). Grass leaf size was associated interactively with MAT and MAP, and with GST and GSP (Extended Data Fig. 3, Supplementary Table 8). The climatic distribution of grass leaf size arises at least in part from exclusion of large-leafed species from dry and cold climates (Extended Data Fig. 4, Supplementary Table 8).

Thermal benefits of small leaf size

We tested three hypotheses for thermal advantages of small leaves for grasses in cold and dry climates using heuristic energy budget modeling[19,20]. First, small leaves may avoid chilling or overheating damage, a mechanism that explains the global biogeographic trend in eudicot leaf size[3]. However, 98% of grass species in the global database had leaves smaller than modelled width thresholds for such damage, i.e., 8.16 and 4.47 cm, respectively[3] and among these species leaf size remained associated with climate (Extended Data Fig. 5), indicating that this mechanism cannot explain the global trend. Second, small leaves, being better coupled with air temperature, may achieve higher light-saturated photosynthetic rate (A) or leaf water use efficiency (WUE) under cold or dry climates[20] (Supplementary Table 9; Extended Data Fig 5). These benefits were supported by model simulations, especially at slower wind speeds; comparing the 5th with the 95th percentile of leaf sizes in our global database, the smaller leaves had 9-27% higher A and/or WUE under cold or dry climates (Supplementary Table 9). Third, smaller leaves may mitigate the short daily and/or seasonal growth period associated with cold and dry regions with a higher A under warm and moist conditions[4], a benefit supported by our simulations, which also showed that smaller leaves had higher transpiration rates (Supplementary Table 9).

Developmental scaling of grass venation

Developmental vein scaling results in strong association of vein traits with grass leaf size. As predicted, globally, smaller leaved species had higher major VLA (r = -0.84 to -0.75, P < 0.001; Fig. 1d, Extended Data Fig. 6). For the 27 grass species grown in the common garden, developmental scaling was supported over the null hypothesis of geometric scaling for numerous vein traits (91 versus 27 of the 111 scaling predictions; P < 0.001; proportion test; Figs. 2-3, Table 1, Extended Data Figs. 6-7, Supplementary Tables 10-11). The diameters of 1° and 2° veins scaled positively with leaf length and area (b = 0.32-0.37; r = 0.61-0.76; P < 0.001; Fig. 2, Extended Data Fig. 6), and the diameters of xylem conduits scaled with their vein diameters (b = 1.3-1.5; r = 0.48-0.65, P < 0.05 – 0.001; Extended Data Fig. 6). The 1° VLA decreased geometrically with increasing leaf width and area (b = -1.0 and -0.56 respectively; r = -1.00 and -0.61, P < 0.001), whereas the 2° VLA decreased less steeply (b = -0.62 and -0.31; r = -0.82 and -0.46, P < 0.05; Fig. 2, Extended Data Fig. 6), and the major and total VLA scaled negatively with leaf width (b = -0.67 and -0.32; r = -0.87 and -0.56, P < 0.01). The diameters of minor veins were independent of leaf length, width and area. The predicted trends of 3° and 4° VLA with leaf length were not significant, but their sum, the total minor VLA, scaled positively with leaf length (b = 0.35-0.36; r = 0.56–0.57, P < 0.01), and was independent of leaf width and area. The vein surface area, projected area and volume per leaf area (VSA, VPA and VVA respectively) also scaled positively with leaf length, and negatively with leaf width, with the exception of only 3° VVA, and all were independent of leaf area (Extended Data Fig. 7). Beyond the predictions of the developmental model, the 5° VLA, VSA and VPA scaled positively with leaf width (r = 0.46-0.57, P < 0.05).

C_3 and C_4 grasses converged in vein scaling (Fig. 2, Extended Data Fig. 8, Supplementary Table 3). C_4 species had more numerous, narrower 3° veins with higher VLA, VSA and VPA, and 7/16 of the C_4 species had 4° veins, resulting in C_4 species having on average almost double the total VLA of the C_3 species. The C_4 species also had narrower 5° veins with lower VSA, VPA, and VVA (P = 0.001 – 0.05).

Hydraulic benefits of small leaf size

Across the 27 grass species grown experimentally, a number of key vein traits were related to species' native climates. Small leaf size and higher major VLA, VSA, VPA and VVA were associated with lower MAP, AI, GSP, and GSL (Supplementary Table 7). Further, tests supported the assumptions based on the published literature (Supplementary Table 4) that C_3 grasses adapted to colder or drier climates have higher light-saturated photosynthetic rates in moist soil, associated with their major vein traits (Extended Data Fig. 9)

Developmental scaling would contribute mechanistically to climate adaptation. Globally, vein scaling trends can explain the absence of leaves larger than 51.4 cm^2 where MAT < 0 °C (Extended Data Fig. 5), as their midrib conduits would be wider than 35 µm (Extended Data Fig. 6), and thereby vulnerable to freeze-thaw embolism[21]. The narrow xylem conduits of small leaves would protect against embolism during drought, and their higher major VLA provides a high capacity flow around blockages, further reducing hydraulic vulnerability to dehydration (Supplementary Table 4)[6,22-25]. The higher major VLA of smaller leaves would also contribute to mitigating shorter growing periods associated with colder, drier climates[11,12], by providing higher hydraulic conductance, enabling the maintenance of open stomata for higher photosynthetic rate despite the higher transpiration loads expected from their thinner boundary layer (Extended Data Fig. 9)[6,26].

Discussion

The worldwide association of small grass leaf size with cold and arid climates arises from millions of years of grass migration and evolution, from the tropics to colder, drier climates and from forest understoreys to open grasslands[8] (Supplementary Table 1). The biophysical and developmental advantages of small grass leaves can explain this pattern. The thinner boundary layer of small grass leaves confers moderately higher photosynthetic rate and water use efficiency in cold and dry climates, and can mitigate shorter growing days and seasons, especially under the very low wind speeds expected for closed, dense stands[27-30]. Their higher major VLA and narrower xylem conduits directly contribute to cold and drought tolerance. The strong climatic association of leaf size and vein traits indicates a substantial importance against the background of other adaptations, including leaf hairs, leaf rolling and mesophyll desiccation tolerance, and beyond leaves, annual vs. perennial life history, stem and root hydraulic adaptation, and root morphology[31-33].

Developmentally-based vein scaling relationships held strongly across diverse grass species, even including those possessing a pseudopetiole, such as bamboos. These relationships may also apply to nongrass species from other families within the Poales. Grass developmental vein scaling relationships were distinct though analogous to those of typical eudicot leaves (Box 1, Figs. 1-2). In eudicots, as expected from their diffuse lamina growth, major vein traits scale negatively with final leaf area (Supplementary Table 4), whereas in grasses, vein traits scale more directly with length or width (Box 1, Table 1, Fig. 2). Yet, for both grasses and eudicots, total VLA, a key determinant of hydraulic capacity and photosynthetic rate[6], was independent of final leaf area. This lack of constraint on total VLA would enable grass diversification in leaf size across environments as for eudicots[5,26,34], as large-leafed grasses, despite their low major VLA, can achieve sufficient hydraulic capacity with their minor vein length to occupy wet, sunny habitats[6 34,35] The decoupling of total VLA from leaf size also enables C_4 species to achieve higher VLA than C_3 species, irrespective of leaf size (Box 1, Fig. 2). However, unlike eudicots[5], in grasses, larger leaves did not have higher VVA, a trait that contributes substantially to leaf construction cost[36], indicating less restriction on their leaf size evolution in resource-rich environments, where larger leaves may confer advantages in light-use efficiency, and by shading other species[37,38]. While the common developmental program across species explains many vein scaling relationships, these may also arise from selection based on function. In longer leaves, larger diameter veins may provide necessary structural and hydraulic support[6,39] In wider leaves, more numerous 5° transverse veins may reinforce against bending[40], and provide hydraulic pathways mitigating their lower major VLA[6]. Similarly, the greater 5° vein diameters in C_3 than C_4 species may compensate for their lower minor VLA (Fig. 2).

The relationships of grass leaf size and vein traits to climate have diverse potential applications. In eudicots, these traits are frequently included for estimating species' adaptation to climate[6], an approach that can be extended to grasses. For grasses, as shown for eudicots[5,41], vein scaling can enable the reconstruction of leaf size fossilized leaf fragments, improving paleoclimate estimation (Extended Data Fig. 10). Anticipating future climate change, leaf size and vein traits can be key targets for grass crop design, which is central to food and biofuel security[42,43]. A current grand challenge is the engineering of C_4 metabolism into C_3 crops such as rice[43], and a higher total VLA has been targeted as a promising step[44,45]. Global trends indicate that C_4 species with narrow leaves and high major VLA would be especially advantaged under the increased temperature and irregular precipitation expected for grasslands[25,46,47].

References

1 Hort, A. *Enquiry into plants, vol. I, by Theophrastus*. (Harvard University Press, 1948).

2 Peppe, D. J. et al. Sensitivity of leaf size and shape to climate: global patterns and paleoclimatic applications. *New Phytol.* **190**, 724-739 (2011).

3 Wright, I. J. et al. Global climatic drivers of leaf size. *Science* **357**, 917-921 (2017).

4 Gates, D. M. Transpiration and leaf temperature. *Ann. Rev. Plant Physio.* **19**, 211-238 (1968).

5 Sack, L. et al. Developmentally based scaling of leaf venation architecture explains global ecological patterns. *Nat. Commun.* **3**, 1-10 (2012).

6 Sack, L. & Scoffoni, C. Leaf venation: structure, function, development, evolution, ecology and applications in the past, present and future. *New Phytol.* **198**, 983-1000 (2013).

7 Beer, C. et al. Terrestrial gross carbon dioxide uptake: Global distribution and covariation with climate. *Science* **329**, 834-838 (2010).

8 Gallaher, T. J. et al. Leaf shape and size track habitat transitions across forest-grassland boundaries in the grass family (*Poaceae*). *Evolution* **73**, 927-946 (2019).

9 Soreng, R. J. et al. A worldwide phylogenetic classification of the *Poaceae* (Gramineae) II: An update and a comparison of two 2015 classifications. *J. Syst. Evol.* **55**, 259-290 (2017).

10 Schuepp, P. H. Tansley review No. 59 Leaf boundary layers. *New Phytol.* **125**, 477-507 (1993).

11 Orians, G. H. & Solbrig, O. T. A cost-income model of leaves and roots with special reference to arid and semiarid areas. *Am. Nat.* **111**, 677-690 (1977).

12 Körner, C. Plant adaptation to cold climates. *F1000 Research* **5**, 1-5 (2016).

13 Niklas, K. J. *Plant Allometry: the scaling of form and process*. (University of Chicago Press, 1994).

14 Nelson, T. & Dengler, N. Leaf vascular pattern formation. *Plant Cell* **9**, 1121-1135 (1997).

15 Christin, P. A. et al. Anatomical enablers and the evolution of C_4 photosynthesis in grasses. *P. Natl. Acad. Sci. USA* **110**, 1381-1386 (2013).

16 Ueno, O., Kawano, Y., Wakayama, M. & Takeda, T. Leaf vascular systems in C_3 and C_4 grasses: A two-dimensional analysis. *Ann. Bot-London* **97**, 611-621 (2006).

17 Sage, R. F. The evolution of C_4 photosynthesis. *New Phytol.* **161**, 341-370 (2004).

18 Clayton, W. D., Vorontsova, M. S., Harman, K. T. & Williamson, H. *GrassBase - The Online World Grass Flore*, <http://www.kew.org/data/grasses-db.html> (2006).

19 Parkhurst, D. F. & Loucks, O. L. Optimal leaf size in relation to environment. *J. Ecol.* **60**, 505-537 (1972).

20 Okajima, Y., Taneda, H., Noguchi, K. & Terashima, I. Optimum leaf size predicted by a novel leaf energy balance model incorporating dependencies of photosynthesis on light and temperature. *Ecol. Res.* **27**, 333-346 (2011).

21 Davis, S. D., Sperry, J. & Hacke, U. The relationship between xylem conduit diameter and cavitation caused by freezing. *Am. J. Bot.* **86**, 1367-1372 (1999).

22 Blackman, C. J., Brodribb, T. J. & Jordan, G. J. Leaf hydraulic vulnerability is related to conduit dimensions and drought resistance across a diverse range of woody angiosperms. *New Phytol.* **188**, 1113-1123 (2010).

23 Scoffoni, C., Rawls, M., McKown, A., Cochard, H. & Sack, L. Decline of leaf hydraulic conductance with dehydration: Relationship to leaf size and venation architecture. *Plant Physiol.* **156**, 832-843 (2011).

24 Scoffoni, C. et al. Leaf vein xylem conduit diameter influences susceptibility to embolism and hydraulic decline. *New Phytol.* **213**, 1076-1092 (2017).

25 Craine, J. M. et al. Global diversity of drought tolerance and grassland climate-change resilience. *Nat. Clim. Change* **3**, 63-67 (2013).

26 Scoffoni, C. et al. Hydraulic basis for the evolution of photosynthetic productivity. *Nat. Plants* **2**, 1-8 (2016).

27 Jones, H. G. *Plants and microclimate : a quantitative approach to environmental Plant Physiol.*. Third edition. edn, (Cambridge University Press, 2014).

28 Grace, J. *Plant-atmosphere relationships*. 1st edn, (Chapman and Hall Ltd, 1983).

29 Weiser, R. L., Asrar, G., Miller, G. P. & Kanemasu, E. T. Assessing grassland biophysical characteristics from spectral measurements. *Remote Sens. Environ.* **20**, 141-152 (1986).

30 Meinzer, F. C. G., D. A. Stomatal control of transpiration from a developing sugarcane canopy. *Plant Cell Environ.* **12**, 635-642 (1989).

31 Liu, H. et al. Life history is a key factor explaining functional trait diversity among subtropical grasses, and its influence differs between C_3 and C_4 species. *J. Exp. Bot.* **70**, 1567-1580 (2019).

32 Fort, F., Jouany, C. & Cruz, P. Root and leaf functional trait relations in *Poaceae* species: Implications of differing resource-acquisition strategies. *J. Plant Ecol.* **6**, 211-219 (2013).

33 Holloway-Phillips, M. M. & Brodribb, T. J. Contrasting hydraulic regulation in closely related forage grasses: implications for plant water use. *Funct. Plant Biol.* **38**, 594-605 (2011).

34 Brodribb, T. J., Feild, T. S. & Sack, L. Viewing leaf structure and evolution from a hydraulic perspective. *Funct. Plant Biol.* **37**, 488-498 (2010).

35 Linacre, E. T. Further notes on a feature of leaf and air temperatures. *Archiv für Meteorologie, Geophysik und Bioklimatologie, Serie B* **15**, 422-436 (1967).

36 John, G. P. et al. The anatomical and compositional basis of leaf mass per area. *Ecol. Lett.* **20**, 412-425 (2017).

37 Givnish, T. J. Comparative studies of leaf form: Assessing the relative roles of selective pressures and phylogenetic constraints. *New Phytol.* **106**, 131-160 (1987).

38 Lusk, C. H., Grierson, E. R. P. & Laughlin, D. C. Large leaves in warm, moist environments confer an advantage in seedling light interception efficiency. *New Phytol.* **223**, 1319-1327 (2019).

39 Olson, M. E. et al. Plant height and hydraulic vulnerability to drought and cold. *P. Natl. Acad. Sci. USA* **115**, 7551-7556 (2018).

40 Niklas, K. J. A mechanical perspective on foliage leaf form and function. *New Phytol.* **143**, 19-31 (1999).

41 Merkhofer, L. et al. Resolving Australian analogs for an Eocene Patagonian paleorainforest using leaf size and floristics. *Am. J. Bot.* **102**, 1160-1173 (2015).

42 Somerville, C. The billion-ton biofuels vision. *Science* **312**, 1277-1277 (2006).

43 Sedelnikova, O. V., Hughes, T. E. & Langdale, J. A. Understanding the genetic basis of C_4 kranz anatomy with a view to engineering C_3 crops. *Ann. Rev. Gen.* **52**, 249-270 (2018).

44 Sage, R. F. & Zhu, X. G. Exploiting the engine of C_4 photosynthesis. *J. Exp. Bot.* **62**, 2989-3000 (2011).

45 Feldman, A. B. et al. Increasing leaf vein density via mutagenesis in rice results in an enhanced rate of photosynthesis, smaller Cell sizes and can reduce interveinal mesophyll cell number. *Front. Plant Sci.* **8**, 1-10 (2017).

46 Edwards, E. J. et al. The origins of C_4 grasslands: Integrating evolutionary and ecosystem science. *Science* **328**, 587-591 (2010).

47 Linder, H. P., Lehmann, C. E. R., Archibald, S., Osborne, C. P. & Richardson, D. M. Global grass (*Poaceae*) success underpinned by traits facilitating colonization, persistence and habitat transformation. *Biol. Rev.* **93**, 1125-1144 (2018).

Main Figure/Display Legends

Fig. 1. Relationships of grass leaf size, traits and species' climatic distribution worldwide. **(a)** Linkages of small leaf size with traits, adaptation to cold and dry climates, and biogeography, as established for eudicotyledons (Supplementary Table 4), and hypothesized for grasses. Small leaves have thin boundary layers (BL), and develop lower major vein diameters (VD_{major}), and higher major vein length per area (VLA_{major}), which provide advantages in cold or dry climates (Supplementary Table 4). Large leaves would be disadvantaged in such climates, relative to warm and moist climates. **(b)** Grass leaf area averaged per country in the global database (across-species mean of leaf area for 21 to 547 species per country; gray when < 20 species represented). **(c)** Grass leaf area in relation to aridity index (where low index signifies a drier climate); each point represents a species (n = 912 C_3 and 840 C_4 species respectively); contour lines and colors represent the 2d kernel density of points. **(d)** The association of major vein length per area (VLA_{major}) with leaf area across grass species (n = 600 species). Statistics represent the fits for

log (y) = log (*a)* + *b* log (x) from ordinary least squares in **(c)** and **(d)**. P = **(c)** 2.3×10^{-27} and **(d)** 1.6×10^{-139} (both two-tailed).

Fig. 2. The scaling of vein traits with leaf dimensions for 27 species of C_3 and C_4 grasses grown in a common garden. (a) – **(d)** Relationships of vein diameters with leaf length and **(e)** – **(h)** of vein lengths per unit leaf area with leaf width: **(a)** & **(e)** first order (1°) veins **(b)** & **(f)** second order (2°) veins **(c)** & **(g)** third order (3°) veins, and, for the species that possess them, fourth order (4°) veins (inset panels) and **(d)** & **(h)** fifth order (5°) transverse veins. Each point represents a species mean value (n = 11 C_3 in white and n = 16 C_4 in gray). Reduced major axis (PRMA) or phylogenetic generalized least square regressions were fitted for log (vein diameter or vein length per area) = log (*a*) + *b* log (leaf length or width), respectively; parameters and goodness of fit in Table 1 and Supplementary Table 10. $^{**}P < 0.01$, $^{***}P < 0.001$; P = **(a)** 0.0007, **(b)** 3.9×10^{-6}, **(e)** 1.2×10^{-34}, **(f)** 1.4×10^{-7} and **(h)** 0.0020 (all two-tailed). Significant trends are plotted with PRMA. Standard errors for species trait values are found in Supplementary Table 3.

Box 1 Fig. 1 Synthetic model for grass leaf ontogeny predicting developmentally-based scaling of vein traits with final leaf size across species. Processes are plotted against developmental phases: phases P and D, formation of the leaf primordium and the cell division zone at the base of the leaf (DZ), respectively; phases D-E and D-E-M, the additions of the expansion zone (EZ) and the maturation zone, resepctively; and phase M, maturation of the whole leaf blade. **(a)** Leaf expansion and the formation of zones; **(b)** Increases of leaf length, width and area; **(c)** Patterning of leaf vein orders from 1° veins to 5° transverse veins for C_3 and C_4 species; some C_4 species develop 4° longitudinal veins ($C_{4\text{-}4L}$ species), whereas C_3 species and $C_{4\text{-}3L}$ species do not; **(d)** Increases in vein length per leaf area and (**e**) in vein diameter for each vein order.

Table 1. Parameters for the scaling of vein diameters and vein lengths per area with mature leaf dimensions across 27 C_3 and C_4 grass species grown in a common garden (*N* = 11 and 16 respectively). Tolerance of cold or dry climates can be conferred by these vein traits and others (vein surface area per leaf area, projected area per leaf area and volume per leaf area,

shown in Supplementary Table 10), as they influence hydraulic capacity and safety, and vascular cost (Supplementary Table 4). Expectations for these across-species scaling relationships were derived from a developmental model, which predicts the allometric slope *b* in the equation log (trait) = log (*a*) + *b* log (mature leaf length, width or area) (Supplementary Table 6), due to intrinsic (*i*) and enabling (*e*) effects (Box 1); expectations from the alternative, geometric scaling model were also derived (Supplementary Tables 6 and 10). Allometric equations were fitted using two-tailed phylogenetic reduced major axis (PRMA) or phylogenetic generalized least squares (PGLS) for the scaling of vein diameter or vein length per area, respectively, with *r*-values and *p*-values, and parameters *a* and *b*, including 95% confidence intervals (CIs) for *b*-values. Bold type indicates that the *b*-values predicted from the developmental model were supported in the experimental, i.e., the scaling relationship across species was significant, and the predicted *b*-value was within the 95% CIs for the observed *b*-value. Significance: *$P < 0.05$, **$P < 0.01$, ***$P < 0.001$, NS: Not significant.

Methods

Testing for the linkage of leaf size and vein traits with climate across grass species worldwide

We extracted data from the Kew Royal Botanic Garden Grassbase, which was compiled from a combination of floristic accounts and publications[18]. We extracted all available data for maximum leaf length, maximum leaf width, maximum 2° vein number, and maximum culm height data, which included values for up to 1752 species depending on the trait (i.e., up to 912 C_3 and 840 C_4 species from 373 genera)[18]. We calculated leaf area by multiplying maximum leaf length by maximum leaf width. We divided the maximum leaf length and maximum 2° vein number respectively by maximum leaf width to determine 1° and 2° vein lengths per area, and summed these to calculate major vein length per area, resulting in values for 616 species for these traits. To test associations of leaf morphological and venation traits with species' native climates, we extracted geographical records from the Global Biodiversity Information Facility web portal (http://www.gbif.org). Species names were checked against the Kew grass synonymy database[18] via the software package Taxonome[48] and The Plant List (http://www.theplantlist.org) via package Taxostand in R[49]. We discarded records if these were duplicates, or names were not recognized in any databases, or the country did not match the coordinates, or coordinates contained fewer than three decimals, or species had fewer than five occurrences. For each location, values for mean annual temperature (MAT), mean annual precipitation (MAP), and mean monthly temperature and precipitation were extracted from WorldClim2 5-arc minute resolution[50], and for aridity index (AI)[51] from CRU TS4.01 01[52]. We also estimated growing season variables, considering growing season months as those with mean temperature ≥ 4 °C and precipitation $\geq 2 \times$ mean monthly temperature; growing season length (GSL) was calculated as the number of those months, growing season temperature (GST) by averaging their mean temperatures, and growing season precipitation (GSP) by summing their mean precipitation[53]. Climate variables were averaged from all given locations for each species. We focused on the relationships of traits with mean climate variables based on the hypothesis that if gene flow occurs among populations of a given species across its native range, that species' mean phenotypic trait values would be related to their mean climate variables[54].

Construction of a synthetic model for grass leaf development, and derivation of allometric predictions based on developmental and geometric scaling

To determine whether leaf development would constrain specific vein traits in smaller leaves, we formulated a synthetic grass leaf developmental model and derived expectations for the relationship of vein traits with final leaf dimensions across species (Box 1, Supplementary Tables 5-6). To construct this model, we conducted searches for previously published studies that included developmental data and/or images of grass leaf development using the keywords "grass leaf development, "grass vein development", "grass histogenesis", "grass morphogenesis", "Poaceae", "leaf ontogeny", "leaf histology, "leaf growth, "leaf anatomy", "vascular development", "vasculature development" in the Web of Science database and the Google Scholar search engine, resulting in a compilation of 61 studies of 20 grass species[14,55-114]. From these studies we extracted key steps in leaf and vein development that were general across species into a synthetic model. Then, given the spatial and temporal constraints arising from development according to this model, we derived expectations for the scaling across species of vein traits with mature leaf size. For instance, the 1° vein length per area declines geometrically with final leaf width (1° VLA = 1/leaf width) as veins are separated by greater numbers of cell divisions and/or by larger cells. By contrast, the 2° VLA declines less steeply than geometrically with final leaf width, as wider leaves may form greater numbers of 2° veins though these will be spaced further apart by subsequent leaf expansion (see Box 1 and Supplementary Table 6 for additional derivations).

Further, as a null hypothesis against which to test developmentally-based scaling predictions, we derived expectations for the relationships of vein traits to leaf dimensions based on geometric scaling[5,13]. Geometric scaling represents the relationships expected among the dimensions of an object given increases in size while maintaining constant proportions and composition. Thus, linear dimensions such as length (L), area (A) and volume (V) would be inter-related as $A \propto L^2$ and $V \propto L^3$. Predictions can then be derived for any other traits based on their dimensions. For instance, given geometric scaling, VLA would be expected to scale with leaf width as VLA $\propto \mathrm{LW}^{-1}$, because VLA, as a linear dimension divided by an area, i.e., L/A, would be related to L/L^2, $= L^{-1}$, whereas LW would scale directly with L. In total, 111 predictions derived from the developmental model were compared with respective predictions from geometric scaling. These 111 predictions included the scaling relationships of five vein diameters (i.e., for each of five vein orders) versus three leaf dimensions (i.e., leaf length, width and area), amounting to 15 predictions; plus the scaling relationships for VLA, VSA, VPA and VVA for each of the five vein orders and for the major, vein, and total vein systems, versus the three leaf dimensions, amounting to $4 \times 8 \times 3 = 96$ predictions. The developmental model predictions for relationships generally differed strongly from those of geometric scaling (i.e., 75% of predictions differed), though, for a few relationships, such as that of 1^{o} VLA with final leaf size, the expectations from developmental scaling and geometric scaling were the same. Overall, developmental scaling predicted that 51 vein traits would scale with leaf size and 60 traits would be independent of leaf dimensions, whereas geometric scaling predicted 63 and 48 respectively (Supplementary Table 6 and 10).

Plant material

To test vein scaling relationships, grasses of 27 diverse species were grown in a common garden to reduce the environmentally-induced plasticity that would occur in wild plants in their native ranges (Extended Data Fig. 2, Supplementary Table 3). While experimental species were selected to encompass large phylogenetic and functional variation, including 11 C_3 species and 16 C_4 species, representing 11 independent C_4 origins, the species necessarily included a only subset of the phylogenetic distribution of the 1752 species in the database analyses of global trait-climate relationships. Seeds were acquired from seed banks and commercial sources (Supplementary Table 3). Prior to germination, seeds were surface-sterilized with 10% NaClO and 0.1% Triton X-100 detergent, rinsed three times with sterile water, and finally sown on plates of 0.8 % agar sealed with Micropore surgical tape (3M, St. Paul, MN). Seeds were germinated in chambers maintained at 26˚C, under moderate intensity cool white fluorescent lighting with a 12 hour photoperiod. When roots were 2-3 cm long, seedlings were transplanted to 3.6 L pots with potting soil (1:1:1.5:1.5:3 of coarse vermiculite: perlite: washed plaster sand: sandy loam: peat moss).

Plants were grown at the UCLA Plant Growth Center (minimum, mean and maximum daily values for temperature: 20.1, 23.4 and 34.0 ^{o}C; for relative humidity: 28, 50 and 65%; and mean and maximum photosynthetically active radiation during daylight period: 107 and 1988 μmol photons m^{-2} s^{-1}; HOBO Micro Station with Smart Sensors; Onset, Bourne, MA), arranged in six randomized blocks spread over three benches, with one individual per species per block and two blocks per bench (*n* = 6 except *n* = 4 for *Alloteropsis semialata*). Plants were irrigated daily with water containing fertilizer (200-250 ppm of 20:20:20 N:P:K; Scotts Peters Professional water soluble fertilizer; Everris International B.V., Geldermalsen, The Netherlands). All species were grown until flowering to confirm species' identities.

Sample anatomical preparation

Leaves were collected when plants had numerous mature leaves, after 2.5 – 7 months of growth, depending on species, given variation in growth rates. Leaves from each of six individuals per species were fixed and stored in FAA solution (37% formaldehyde-glacial acidic acid-95% ethanol in deionized water). Transverse sections were made for one leaf from each of three individuals. Rectangular samples were cut from the center of leaves halfway along the length of the blade and gradually infiltrated under vacuum with low viscosity acrylic resin for one week (L.R. White; London Resin Co., UK), and set in resin in gelatin capsules to dry at 55 °C overnight. Transverse cross sections 1 µm in thickness were prepared using glass knives (LKB 7800 KnifeMaker;LKB Produkter; Bromma, Sweden) in a rotary microtome (Leica Ultracut E, Reichert-Jung California, USA), placed on slides, and stained with 0.01% toluidine blue in 1% sodium borate (w/v). Slides were imaged with a light microscope using a 5×, 20×, and 40× objective (Leica Lietz DMRB; Leica Microsystems) and camera with imaging software (SPOT Imaging Solution; Diagnostic Instruments, Sterling Heights, Michigan USA). Additionally, one leaf from each of three individuals was used to prepare chemically cleared leaf sections to visualize veins. Square sections of 1 cm × 1 cm were cut from the center of the leaf at the widest point, cleared with 5 % NaOH in ethanol, stained with safranin, and counterstained with fast-green[115]. Sections were mounted with water in transparency film (CG5000; 3M Visual Systems Division) and scanned (flatbed scanner; Canon Scan Lide 90; 1,200 pixels per inch), and further imaged with a light microscope using a 5× and 10× objective.

Quantification of leaf dimensions and vein traits

Leaf dimensions tested were leaf width, leaf length, and leaf area, with leaf width and leaf length measured at the widest and longest regions of the leaf respectively. Leaf area was calculated as leaf length × leaf width[116-118]. Estimates of leaf area from length and width can be improved by multiplying by a correction factor constant, which has been proposed as 0.7-0.9 for grasses[116-118], but as there is no standard value, we did not apply such a correction factor. Applying a constant correction factor would have no influence on correlations or regression fits or their statistical significance for trait-climate relationships. Further, applying a constant correction factor would not influence the tests of scaling of vein traits with leaf area, which focused on power law scaling exponents; multiplying estimates of leaf area by a constant would result only in change to the power law scaling intercept, and not the exponent. Thus, applying a correction factor to leaf area, or not, would have no influence any of the findings of our study.

We measured and analyzed cross sections of one leaf for each of three individuals per species, to quantify the diameters and numbers of veins in the transverse plane for all vein orders, excluding 5° veins, which generally were not visible in transverse sections, and for which we used the chemically cleared and stained leaf sections. Vein orders were established for each species based on vein size, presence/absence of enlarged metaxylem, and presence/absence of fibrous tissue above or below the vein[119,120]. The 1° vein or midvein was the large central vein containing the largest metaxylem and fibrous tissue, and the 2° veins were the "large" veins that were substantially smaller than the midvein and of similar structure. We identified the minor veins as the smaller veins, i.e., the 3° "intermediate" and 4° "small" veins, and perpendicular 5° transverse veins[120]. Notably, 4° veins occur only in NADP-ME C_4 grasses of the subfamily Panicoideae (7/16 of the C_4 species)[15], and can be distinguished based on their smaller overall size than 3° veins and their absence of sclerenchyma strands. For the species *Lasiacis sorghoidea*, 2° veins were too few to be counted in our prepared transverse sections, and we established vein orders and quantified associated traits using the chemically cleared and stained leaves.

For each vein order, the vein length per area (VLA) was quantified as the vein number per leaf width (cm^{-1} or mm^{-1}), which is equivalent to vein length per unit leaf area (same units), assuming an approximately rectangular leaf. Cross-sectional vein diameters (VD) were measured excluding the bundle and mestome sheath cell layers, and averaging horizontal and vertical axes. Cross-sectional diameters were measured for all xylem conduits in each vein order by considering the lumen cross-sections as ellipses and averaging the major and minor axes. We categorized two metaxylem types within major veins, based on their highly distinct sizes (i.e., large and small metaxylem), and one metaxylem type for minor veins (i.e., "small metaxylem"). We focused on the large metaxylem conduits within major veins in calculating average conduit diameter values, as these would contribute the bulk of maximum flow[121,122]. For *Lasiacis sorghoidea*, as 2° veins were too few to be counted from our prepared transverse sections, we could not quantify the conduits within these veins and thus analyses of 2° vein conduit dimensions excluded this species.

For all vein orders, we estimated vein surface per unit leaf area (VSA), vein projected area per unit leaf area (VPA), and vein volume per unit leaf area (VVA)[5]:

$$\mathrm{VSA} = \mathrm{VLA} \times \pi \times \mathrm{VD} \tag{2}$$

$$\mathrm{VPA} = \mathrm{VLA} \times \mathrm{VD} \tag{3}$$

$$\mathrm{VVA} = \mathrm{VLA} \times \pi \times (\mathrm{VD}/2)^2 \tag{4}$$

Determination of vein allometries, and testing against predictions from developmental and geometric scaling

We determined trait scaling relationships by fitting lines to log-transformed data. The relationship of each vein trait (y) to a given leaf dimension (x) was considered as an allometric power law:

$$\mathrm{y} = a\mathrm{x}^{b} \tag{5}$$

$$\log(\mathrm{y}) = \log(a) + b\log(\mathrm{x})$$

where b is the scaling exponent.

We tested these relationships against the predictions from developmentally-based scaling derived from the synthetic leaf developmental model (see "*Construction of a synthetic model for grass leaf development, and derivation of allometric predictions based on developmental and geometric scaling*" and Box 1, Table 1, and Supplementary Table 6)[5]. A scaling relationship was considered to be consistent with a prediction if its 95% confidence intervals included the predicted slope. We tested whether a greater proportion of predictions were explained by developmental scaling than by geometric scaling using a proportion test (Minitab 16; State College, Pennsylvania, USA).

Testing assumptions for the linkages of photosynthetic rate with climate and vein traits

For the grass species grown experimentally, light-saturated rates of photosynthesis were measured for plants in moist soil, enabling a test of the assumptions that C_3 grass species from arid or cold environments have high photosynthetic rates, and that photosynthetic rate would be related to vein length and surface area per leaf area. Light-saturated rates of photosynthesis were measured from 17 Feb to 28 June 2010, between 0900 and 1500, on a mature leaf on each plant for six plants per species. Measurements were taken of steady state gas exchange (< 2% change over six minutes) using a LI-6400 XT portable photosynthesis system (LI-COR, Lincoln, Nebraska, USA). Conditions within the leaf chamber were set to 25°C, with reference CO_2 400 ppm, and PPFD 2000 µmol m^{-2} s^{-1}, and the relative humidity was 60-80%, resulting in vapor pressure deficits (VPD) of 0.80-1.6 kPa. Measurements were made on 1-2 leaves from each of 6 plants (except *L. sorghoidea*, 3 leaves from each of two plants). 5-9 leaves per species were measured, with 6 on average. Leaves were harvested and scanned for leaf area (Canon Scan Lide 90, Canon USA, Lake Success, NY). Leaf-area normalized values were determined for net light-saturated photosynthetic rate per leaf area (A_{area}).

In addition, we tested for even stronger general support of the relationships of photosynthetic rate with climate variables by combining our data for 8 C_3 terrestrial species with data for 13 Northern Hemisphere temperate terrestrial C_3 grass species from the GLObal Plant trait NETwork (GLOPNET) database[123], for which photosynthesis, latitude and longitude data for their field site were available (Supplementary Table 12). We extracted climate variables mean annual temperature (MAT), mean annual precipitation (MAP), and monthly temperature and precipitation to calculate growing season length (GSL) (see *Testing for the linkage of leaf size and vein traits with climate across grass species worldwide* above for methods of calculation), based on the latitude and longitude from which each species was measured.

Phylogenetic reconstruction

A phylogenetic hypothesis for the 27 experimentally grown species considered in this study was inferred from three markers from the chloroplast genome (*rbcL*, *ndhF* and *trnKmatK*), available for the exact same accessions in published datasets[124,125]. Each marker was aligned individually using MUSCLE[126], and the alignments were manually refined. The total dataset was 6179 bp long. The program BEAST[127] was used to obtain a time-calibrated phylogeny under a relaxed clock model with uncorrelated evolutionary rates that follow a log-normal distribution. The substitution model was set to a general time reversible model with a gamma-shape parameter and a proportion of invariants. The root of the tree (split of BOP and PACMAD clades) was forced to follow a normal distribution with a mean of 51.2 Ma and a standard deviation of 0.0001 Ma, based on previous estimates[128]. The addition of phytolith fossils would alter the absolute ages estimated by molecular dating[129], but the relative ages would remain unchanged and the comparative analyses consequently would be unaffected. Two parallel analyses were run for 10,000,000 generations, sampling a tree every 1,000 generations. Median ages across the 18,000 trees samples are a burn-in period of 1,000,000 generations were mapped on the maximum credibility tree. The burn-in period was largely sufficient for the analysis to reach stability, as verified with the program Tracer (http://beadt.bio.ed.ac.uk/Tracer).

Using the R Language and Environment version 3.4.1[130] with the ape R package[131] a phylogenetic hypothesis for 1752 of the Grassbase species was extracted from a published phylogeny available through Dryad[132]. The source phylogeny assessed relationships among 3595 species using a set of 14 sub trees using various genetic datasets in combination with three core plastid markers *rbcL*, *ndhF* and *matK*, with dating based on macrofossil evidence[9].

Testing trait-climate associations

To test trait-climate associations, we quantified the strength of correlations using Pearson *r* rather than fitting specific predictive regression equations with R^2 values. For trait-climate associations we calculated both ahistorical correlations and relationships accounting for phylogenetic relatedness (PGLS or PRMA, see section *Comparative analyses* below). While the phylogenetic analyses more robustly test our evolutionary hypotheses, the ahistorical Pearson *r* values better resolve the strengths of existing relationships across species, especially when trends arise from variation among groups that split in evolution deep in the phylogeny[133]. In both types of analysis, the *r* values provide a conservative estimate of trait-climate relationships. As in previous biogeographic trait-climate analyses[134,135], we related species' average trait values from a database or experimental measurements to modelled native climates based on natural occurrences; relationships would be yet stronger if traits and climate were matched for individual plants[136]. Additionally, the modelled native climates do not account for variation to which species would be adapted in the field in temperature, irradiance and water availability due to microclimate associated with topography and canopy cover, or soil characteristics; accounting for this variation would likely improve the strength of trait-climate relationships[136]. Overall, global associations of traits with climate that were supported by substantial, statistically significant ahistorical *r* values indicate robust, biologically significant relationships, and significant phylogenetic correlations additionally indicate support for the evolutionary hypotheses[137,138].

We implemented several further analyses to resolve the associations of traits with climate in the worldwide grass trait database. We conducted phylogenetic multiple regression to test for significant interactive effects of temperature and precipitation on leaf traits. Models including MAT and MAP (or GST and GSP) alone or in combination, and including an interaction were compared using Akaike Information Criterion (AIC)[139]. Prior to phylogenetic multiple regression analyses, MAP values were divided by 50 to achieve a similar scale of values as MAT, and GSP values were divided by 100 to achieve a similar scale of values as GST. Plant traits, MAP and MAT were then log transformed, and MAT and MAP (and GST and GSP) were centered by subtracting the mean to render coefficients of main effects and interaction terms biologically interpretable[140].

The parametric correlation and regression statistics calculated in this study are subject to assumptions, i.e., independence of observations, and the normal distribution and homoscedasticity of residuals[141]. Evolutionary non-independence among species was adjusted for using phylogenetic statistics[133]. To check that the assumptions of normality and heteroscedasticity did not influence statistical significance of univariate analyses, we checked for significance of Spearman's rank correlations, which are not subject to these assumptions, and confirmed as significant ($p < 0.05$) the relationships presented in the text. For the multiple regression of leaf area versus MAT and MAP in the 1752 species global database, the 29 species with MAT < 0 °C resulted in a left-skew of log-transformed MAT and a notable heteroscedasticity of residuals (Supplementary Fig. 1). To confirm that this skew did not influence the findings of the multiple regressions, we repeated the analysis excluding the 29 species, which alleviated the skew and heteroscedasticity (Supplementary Fig. 2); the key finding of the multiple regression analysis, i.e., the interactive effect of MAT and MAP, was unaffected (Supplementary Table 8). Notably, the multiple regression analysis of leaf area versus growing season temperature and growing season precipitation also confirmed the trend, with greater normality and homoscedasticity of residuals, both when including all 1752 species and when excluding the 29 species with MAT < 0 °C (Supplementary Tables 7 and 8; Supplementary Figs. 3-4).

We conducted hierarchical partitioning analyses on log transformed data to resolve the independent statistical associations of leaf size with individual climate variables[142]. Finally, we distinguished whether trait-climate correlations can be partially explained due to "triangular relationships", i.e., when data are missing in one or more corners of the plot, an analysis that can provide special insights[143,144]. For example, a positive trait-climate correlation would arise at least in part from a triangular relationship if high trait values are few or absent at lower values of the climate variable, or if low trait values are few or absent at high values of the climate variable. To test for the presence of triangular relationships, we implemented quantile regression analyses, determining regression slopes fitted through the 5%, 50% and 95% quantiles of log transformed data[145-147]. A triangular relationship was supported when the regressions through the 95% and 5% quantiles differed according to *t*-tests.

Comparative analyses

Comparative phylogenetic statistical analyses accounting for the effects of phylogenetic covariance on trait-climate and trait-trait relationships were conducted using the R Language and Environment version 3.4.1[130].

Regression coefficients were estimated using phylogenetic least squares (PGLS) and/or phylogenetic reduced major axis (PRMA), in each case basing the phylogenetic correction on Pagel's λ[148,149] estimated by maximum likelihood[150]. For PGLS, corPagel[151] was used in combination with gls[150] and optimized[131] to establish maximum likelihood estimates of λ in the 0 – 1 range; for PRMA, phyl.RMA[151] was used. Confidence intervals for *b* estimated using PRMA were determined following ref[152]:

$$\pm\hat{b}\left(\sqrt{B+1}\pm\sqrt{B}\right), where B = \frac{1-r^2}{N-2} f_{1-\alpha,1,N-2}$$

where $\hat{b}$ is the fitted value for *b*; r is a correlation coefficient, for which we used a phylogenetically corrected estimate based on the variance-covariance matrix output by phyl.RMA; *N* is the number of pairs of observations; and $f_{1-\alpha,1,N-2}$ is the critical value from the F distribution.

Differences in species-level trait means between C_3 and C_4 species were tested using a phylogenetically corrected ANOVA, both parametric (based on phylogenetic generalized least squares analysis, PGLS) and nonparametric[153]; *phyloANOVA* in R package[151].

The impact of phylogenetic corrections was evaluated by comparing PGLS or PRMA with Pagel's λ estimated by maximum likelihood, to equivalent models in which Pagel's λ was set to 0. When using Pagel's λ, to assess normality and homoscedasticity assumptions we first extracted phylogenetic residuals. For PGLS, the function *residuals* was used to extract normalized residuals; for PRMA, a custom code (available on request), derived from an original provided by Professor Robert P. Freckleton, was used to produce an equivalent transformation of raw residuals obtained from *phyl.RMA*. Normality was tested using Anderson Darling tests[154] and heteroscedasticity using Bartlett's test[130]. Additionally, PGLS was used to estimate Pagel's λ for phylogenetic residuals, which should be 0.

The PGLS and PRMA approaches used to test for scaling relationships of vein traits with leaf dimensions and to estimate the slopes of linearized power law relationships are phylogenetic approaches equivalent to ordinary least squares and reduced major axis regressions, respectively. Which of the two was used depended on the specific relationship tested. The least squares approach is preferable in cases when a dependent Y variable is related to an independent X variable, specifically when (1) there is much less error (i.e., natural variation and/or measurement error) in X than Y, and/or when (2) conceptually, Y is causally determined by, or to be predicted from, X, but never X from Y[155,156]. By contrast, the reduced major axis approach is preferable in cases when (1) X and Y have similar error, and/or when (2) X or Y are co-determined, or their relationship arises from an underlying functional coordination, or either could reasonably be predicted using the other; this approach is typically used in studies of allometric scaling relationships among functional traits or organ dimensions[155,156]. An exception to the use of reduced major axis for allometry is when testing whether the allometric slope of a relationship is consistent with an expected slope that was derived algebraically from other equations, as only least-squares slopes are robust to algebraic manipulation[156]. For example, PGLS would be selected over PRMA to test an expectation for the scaling slope of vein surface area per leaf area (VSA) with leaf length, that was derived algebraically by multiplying the expected scaling slopes of vein length per area (VLA) and vein diameter (VD) with leaf length, given that VSA is determined from VLA and VD (see, "*Quantification of leaf dimensions and vein traits*", above). Further, while least squares is appropriate for testing relationships of a dependent versus an independent trait, reduced major axis can be preferable for illustrating the relationship in a plot, given that it captures more closely the central trend among two variables with high and/or similar error[155,156].

Thus, we selected PGLS or PRMA for the tested relationships according to which was most appropriate given the above principles, while noting that the application of any single approach globally would not affect the findings of the study, but would reduce the accuracy of the specific slope estimates. We used PRMA to test relationships of traits with climate variables, as the magnitude of variation in modelled climate variables globally was similar to that for species means for leaf traits. We also used PRMA for testing scaling relationships of vein diameters with leaf length and width, and of xylem conduit diameters with vein diameters, given the preference of this approach for testing allometric relationships, and the similar error in the X and Y variables. We used PGLS for testing relationships of vein lengths, surface areas and volumes per leaf area with leaf dimensions, given the higher variability in the vein traits than leaf dimensions arising due to their determination from one or more vein traits as well as leaf dimensions (e.g., vein length per leaf area = vein number / leaf width). Further, PGLS was most appropriate for testing allometric slopes for the relationships of vein traits to leaf area, because the expectations for these slopes from the developmental model were derived algebraically from expected slopes of vein traits in relation to leaf length and leaf width[155]. Finally, we used PRMA in all figure plots to most clearly illustrate the central trends accounting for phylogeny[155,156].

Lastly, we evaluated whether the scaling of vein traits with leaf dimensions differed between C_3 and C_4 species. C_3 and C_4 species were considered to differ significantly in trait-trait or trait-climate associations if significant relationships were found independently for both groups, and if there was no overlap in scaling slope 95% confidence intervals (CIs) using the selected regression approach (PGLS or PRMA).

Modelling the impacts of leaf energy budget and testing hypotheses for the benefits of smaller leaves under different climates

We considered three hypotheses for the advantage of small leaf sizes in cold or dry climates based on their thinner boundary layer. Smaller leaves have been hypothesized to (1) experience less damage under extreme temperatures, i.e. chilling on colds nights and overheating on hot days[3,157,158], (2) maintain higher rates of photosynthesis and/or higher leaf water use efficiency in cold and/or dry conditions[19,20] and (3) achieve higher gas exchange in favorable, warm and wet climates[4], which would provide an advantage in mitigating the shorter diurnal and/or seasonal growing periods of cold or dry climates.

To test hypothesis (1), i.e., that small grass leaves are typical in cold or dry climates globally because they avoid extreme temperatures, we calculated the minimum threshold of leaf size for chilling or overheating. We used the 100 cm^2 leaf size threshold for damage by nighttime chilling and 30 cm^2 for damage by daytime overheating, i.e., the lowest thresholds that were modelled for eudicotyledons globally given in Fig. 3 of ref. 3. Those leaf size thresholds for eudicotyledons were derived from estimated damage thresholds based on the "characteristic dimension" of the leaf (d, i.e., the diameter of the largest circle that can be delimited within a leaf) of 8.16 cm and 4.47 cm, according to eqn 4 in the supplemental information of ref 3 ($LA = 1.5\ d^2$). Thus, we used these threshold values to exclude species with leaf width < 8.16 cm and < 4.47 cm, and then tested whether the observed trends of leaf dimensions with MAT and MAP globally remained. Significant trends for this restricted species set would indicate that thresholds for leaf damage under extreme temperatures cannot explain trends for grasses with leaves smaller than those thresholds. By testing trends against these very low thresholds, we provided a very conservative test to establish that avoidance of extreme temperatures would not explain the global climatic distribution of grass leaf size.

To test hypotheses (2) and (3), we used heuristic leaf energy balance modelling to simulate the consequences for gas exchange of leaf sizes varying in size[159]. Using the Tealeaves R package[159], given inputs of leaf width, wind speed, stomatal conductance and air temperature, we simulated boundary layer conductance, leaf temperature, and transpiration rate. To represent the bulk of the global range of grass leaf size, we focused on comparing the global 5^{th} and 95^{th} quantiles of leaf width (0.1 cm and 2.7 cm). We simulated leaves in wet and dry conditions by setting stomatal conductance values at 0.4 mol m^{-2} s^{-1} and 0.2 mol m^{-2} s^{-1}, respectively[160]; our tests showed that selecting other values would yield similar qualitative results. To represent warm and cold climates we simulated gas exchange under air temperatures of 315 K and 280 K (41.85 °C and 6.85 °C respectively)[161]. All other physical and environmental inputs were maintained constant at typical values[159]. We used the output values of leaf temperature and boundary layer conductance to simulate C_3 photosynthetic rate for leaves of different widths using the Farquhar model[162,163]. We tested these effects at the two wind speeds, 0.1 m/s and 2 m/s. Lastly, we tested simulations for both amphistomatous and hypostomatous leaves, and we present results for amphistomatous leaves given that most grasses are amphistomatous[164]. To test for the potential benefit of smaller leaves, we calculated the ratios of photosynthetic rate, transpiration and leaf water use efficiency for a small relative to large leaf; values > 1 indicate an advantage for the small leaf in cold or dry conditions. To test for the potential benefit of smaller leaves in mitigating a shorter period with favourable climate, we calculated the ratios of photosynthetic rate, transpiration and leaf water use efficiency under warm and wet conditions for a small versus a large leaf; again, values > 1 signify a small leaf advantage.

Supplementary References

48 Kluyver, T. A. & Osborne, C. P. Taxonome: a software package for linking biological species data. *Ecol. Evol.* **3**, 1262-1265 (2013).

49 Cayuela, L., Granzow-de la Cerda, I., Albuquerque, F. S. & Golicher, D. J. TAXONSTAND: An R package for species names standardisation in vegetation databases. *Methods Ecol. Evol.* **3**, 1078-1083 (2012).

50 Fick, S. E. & Hijmans, R. J. WorldClim 2: new 1-km spatial resolution climate surfaces for global land areas. *Int J. Climatol.* **37**, 4302-4315 (2017).

51 Cherlet, M. H., C.; Reynolds, J.; Hill, J.; Sommer, S.; von Maltitz, G. *World Atlas of Desertification*. 3rd edn, (Publication Office of the European Union, 2018).

52 Harris, I., Jones, P. D., Osborn, T. J. & Lister, D. H. Updated high-resolution grids of monthly climatic observations - the CRU TS3.10 Dataset. *Int. J. Climatol.* **34**, 623-642 (2014).

53 Lasky, J. R. et al. Characterizing genomic variation of Arabidopsis thaliana: the roles of geography and climate. *Mol. Ecol.* **21**, 5512-5529 (2012).

54 Sexton, J. P., McIntyre, P. J., Angert, A. L. & Rice, K. J. Evolution and Ecology of Species Range Limits. *Ann. Rev. Ecol. Evol. & Syst.* **40**, 415-436 (2009).

55 Dengler, N. G., Dengler, R. E. & Hattersley, P. W. Differing ontogenetic origins of PCR (Kranz) sheaths in leaf blades of C_4 grasses (*Poaceae*). *Am. J. Bot.* **72**, 284-302 (1985).

56 Dengler, N. G., Woodvine, M. A., Donnelly, P. M. & Dengler, R. E. Formation of vascular pattern in developing leaves of the C_4 grass *Arundinella hirta*. *Int. J. Plant Sci.* **158**, 1-12 (1997).

57 Ikenberry, G.-J. J. *Developmental vegetative morphology of avena sativa* PhD thesis, Iowa State University, (1959).

58 Kaufman, P. B. & Brock, T. G. Structural development of the oat plant. *Agronomy Monograph* **33**, 53 - 75 (1992).

59 Hitch, P. A. & Sharman, B. C. Initiation of procambial strands in leaf primordia of *Dactylis glomerata L* as an example of a temperate herbage grass. *Ann. Bot-London* **32**, 153-164 (1968).

60 Davidson, J. L. & Milthorpe, F. L. Leaf growth in *Dactylis glomerata* following defoliation. *Ann. Bot-London* **30**, 173-184 (1966).

61 Volenec, J. J. & Nelson, C. J. Cell dynamics in leaf meristems of contrasting tall fescue genotypes. *Crop Sci* **21**, 381-385 (1981).

62 Macadam, J. W. & Nelson, C. J. Specific leaf weight in zones of cell division, elongation and maturation in tall fescue leaf blades. *Ann. Bot-London* **59**, 369-376 (1987).

63 Macadam, J. W., Volenec, J. J. & Nelson, C. J. Effects of nitrogen on mesophyll cell division and epidermal cell elongation in tall fescue leaf blades. *Plant Physiol.* **89**, 549-556 (1989).

64 Skinner, R. H. & Nelson, C. J. Elongation of the grass leaf and its relationship to the phyllochron. *Crop Sci.* **35**, 4-10 (1995).

65 Skinner, R. H. & Nelson, C. J. Epidermal cell division and the coordination of leaf and tiller development. *Ann. Bot-London* **74**, 9-15 (1994).

66 Maurice, I., Gastal, F. & Durand, J. L. Generation of form and associated mass deposition during leaf development in grasses: a kinematic approach for non-steady growth. *Ann. Bot-London* **80**, 673-683 (1997).

67 Durand, J. L., Schaufele, R. & Gastal, F. Grass leaf elongation rate as a function of developmental stage and temperature: Morphological analysis and modelling. *Ann. Bot-London* **83**, 577-588 (1999).

68 Martre, P., Durand, J. L. & Cochard, H. Changes in axial hydraulic conductivity along elongating leaf blades in relation to xylem maturation in tall fescue. *New Phytol.* **146**, 235-247 (2000).

69 Martre, P. & Durand, J. L. Quantitative analysis of vasculature in the leaves of *Festuca arundinacea* (*Poaceae*): Implications for axial water transport. *Int. J. Plant Sci.* **162**, 755-766 (2001).

70 Gallagher, J. N. Field studies of cereal leaf growth 1. Initiation and expansion in relation to temperature and ontogeny. *J Exp Bot* **30**, 625-636 (1979).

71 Gallagher, J. N. & Biscoe, P. V. Field studies of cereal leaf growth 3. Barley leaf extension in relation to temperature, orradiance, and water potential. *J. Exp. Bot.* **30**, 645-655 (1979).

72 Dannenhoffer, J. M., Ebert, W. & Evert, R. F. Leaf vasculature in barley, *Hordeum vulgare* (*Poaceae*). *Am. J. Bot.* **77**, 636-652 (1990).

73 Dannenhoffer, J. M. & Evert, R. F. Development of the vascular system in the leaf of barley (*Hordeum vulgare* L). *Int. J. Plant Sci.* **155**, 143-157 (1994).

74 Trivett, C. L. & Evert, R. F. Ontogeny of the vascular bundles and contiguous tissues in the barley leaf blade. *Int. J. Plant Sci.* **159**, 716-732 (1998).

75 Soper, K. & Mitchell, K. J. The developmental anatomy of perennial ryegrass (*Lolium perenne* L.). *NZ J. Sci. Tech.* **37**, 484-504 (1956).

76 Schnyder, H., Nelson, C. J. & Coutts, J. H. Assessment of spatial distribution of growth in the elongation zone of grass leaf blades. *Plant Physiol.* **85**, 290-293 (1987).

77 Arredondo, J. T. & Schnyder, H. Components of leaf elongation rate and their relationship to specific leaf area in contrasting grasses. *New Phytol.* **158**, 305-314 (2003).

78 Kaufman, P. B. Development of the shoot of *Oryza sativa* L. - II. Leaf histogenesis. *Phytomorphology* **9**, 277-311 (1959).

79 Yamazaki, K. Studies on the leaf formation in rice plants: I. Observation on the successive development of the leaf. *Jap. J. Crop Sci.* **31**, 371-378 (1963).

80 Chonan, N. K., H.; Matsuda, T. Morphology on vascular bundles of leaves in gramineous crops: I. Observations on vascular bundles of leaf blades, sheaths and internodes in riceplants. *Jap. J. Crop Sci.* **43**, 425-432 (1974).

81 Hoshikawa, K. *The growing rice plant: an anatomical monograph*. (Nobunkyo, 1989).

82 Matsukura, C. et al. Transverse vein differentiation associated with gas space formation - Fate of the middle cell layer in leaf sheath development of rice. *Ann. Bot-London* **85**, 19-27 (2000).

83 Itoh, J. et al. Rice plant development: from zygote to spikelet. *Plant Cell Physiol.* **46**, 23-47 (2005).

84 Sakaguchi, J. & Fukuda, H. Cell differentiation in the longitudinal veins and formation of commissural veins in rice (*Oryza sativa)* and maize (*Zea mays*). *J. Plant Res.* **121**, 593-602 (2008).

85 Parent, B., Conejero, G. & Tardieu, F. Spatial and temporal analysis of non-steady elongation of rice leaves. *Plant Cell Environ.* **32**, 1561-1572 (2009).

86 Begg, J. E. & Wright, M. J. Growth and development of leaves from intercalary meristems in *Phalaris arundinacea* L. *Nature* **194**, 1097-1098 (1962).

87 Colbert, J. T. & Evert, R. F. Leaf vasculature in sugarcane (*Saccharum officinarum* L). *Planta* **156**, 136-151 (1982).

88 Bernstein, N., Silk, W. K. & Lauchli, A. Growth and development of sorghum leaves under conditions of NaCl stress - Spatial and temporal aspects of leaf growth inhibition. *Planta* **191**, 433-439 (1993).

89 Sud, R. M. & Dengler, N. G. Cell lineage of vein formation in variegated leaves of the C_4 grass *Stenotaphrum secundatum*. *Ann. Bot-London* **86**, 99-112 (2000).

90 Sharman, B. C. & Hitch, P. A. Initiation of procambial strands in leaf primordia of bread wheat *Triticum aestivum* L. *Ann. Bot-London* **31**, 229-243 (1967).

91 Blackman, E. The morphology and development of cross veins in the leaves of bread wheat (*Triticum aestivum* L.). *Ann. Bot-London* **35**, 653-665 (1971).

92 Kemp, D. R. The location and size of the extension zone of emerging wheat leaves. *New Phytol.* **84**, 729-737 (1980).

93 Paolillo, D. J. Protoxylem maturation in the seedling leaf of wheat. *Am. J. Bot.* **82**, 337-345 (1995).

94 Beemster, G. T. S. & Masle, J. The role of apical development around the time of leaf initiation in determining leaf width at maturity in wheat seedlings (*Triticum aestivum* L.) with impeded roots. *J. Exp. Bot.* **47**, 1679-1688 (1996).

95 Sharman, B. C. Developmental anatomy of the shoot of *Zea mays* L. *Ann. Bot-London* **6**, 245-282 (1942).

96 Esau, K. Ontogeny of the vascular bundle in *Zea mays*. *Hilgardia* **15**, 327-368 (1943).

97 Bosabalidis, A. M., Evert, R. F. & Russin, W. A. Ontogeny of the vascular bundles and contiguous tissues in the maize leaf blade. *Am. J. Bot.* **81**, 745-752 (1994).

98 Poethig, S. in *Contemporary problems in plant anatomy* (ed R. A.; Dickison White, W. C.) (Academic Press, 1984).

99 Russell, S. H. & Evert, R. F. Leaf Vasculature in *Zea mays*-L. *Planta* **164**, 448-458 (1985).

100 Smith, L. G., Greene, B., Veit, B. & Hake, S. A dominant mutation in the maize homeobox gene, knotted-1, causes its ectopic expression in leaf-cells with altered fates. *Development* **116**, 21-& (1992).

101 Fournier, C. & Andrieu, B. A 3D architectural and process-based model of maize development. *Ann. Bot-London* **81**, 233-250 (1998).

102 Muller, B., Reymond, M. & Tardieu, F. The elongation rate at the base of a maize leaf shows an invariant pattern during both the steady-state elongation and the establishment of the elongation zone. *J. Exp. Bot.* **52**, 1259-1268 (2001).

103 Muller, B. et al. Association of specific expansins with growth in Maize leaves is maintained under environmental, genetic, and developmental sources of variation. *Plant Physiol.* **143**, 278-290 (2007).

104 Johnston, R., Leiboff, S. & Scanlon, M. J. Ontogeny of the sheathing leaf base in maize (Zea mays). *New Phytol.* **205**, 306-315 (2015).

105 Benhajsalah, H. & Tardieu, F. Temperature affects expansion rate of maize leaves without change in spatial distribution of cell length - Analysis of the coordination between cell division and cell expansion. *Plant Physiol.* **109**, 861-870 (1995).

106 Tardieu, F., Reymond, M., Hamard, P., Granier, C. & Muller, B. Spatial distributions of expansion rate, cell division rate and cell size in maize leaves: a synthesis of the effects of soil water status, evaporative demand and temperature. *J. Exp. Bot.* **51**, 1505-1514 (2000).

107 Runions, A. et al. Modeling and visualization of leaf venation patterns. *Acm T. Graphic* **24**, 702-711 (2005).

108 Scarpella, E. & Meijer, A. H. Pattern formation in the vascular system of monocot and dicot plant species. *New Phytol.* **164**, 209-242 (2004).

109 Baskin, T. I. Anisotropic expansion of the plant cell wall. *Ann. Rev. Cell. Dev.* **21**, 203-222 (2005).

110 Fujita, H. & Mochizuki, A. The origin of the diversity of leaf venation pattern. *Dev. Dyn.* **235**, 2710-272 (2006).

111 Granier, C. & Tardieu, F. Multi-scale phenotyping of leaf expansion in response to environmental changes: the whole is more than the sum of parts. *Plant Cell Environ.* **32**, 1175-1184 (2009).

112 Scarpella, E., Barkoulas, M. & Tsiantis, M. Control of leaf and vein development by auxin. *Csh Perspect Biol* **2** (2010).

113 Gazquez, A. & Beemster, G. T. S. What determines organ size differences between species? A meta-analysis of the cellular basis. *New Phytol.* **215**, 299-308 (2017).

114 Scarpella, E. The logic of plant vascular patterning. Polarity, continuity and plasticity in the formation of the veins and of their networks. *Curr. Opin. Genet. Dev.* **45**, 34-43 (2017).

115 Berlyn, G. P. M., J. P. *Botanical Microtechnique and Cytochemistry*. (Iowa State University Press, 1976).

116 Kemp, C. D. Methods of estimating leaf area of grasses from linear measurements. *New. Phytol.* **24**, 491-299 (1960).

117 Stickler, F. C., Wearden, S. & Pauli, A. W. Leaf area determination in grain sorghum. *Agronony* **53**, 187-188 (1961).

118 Shi, P. et al. Leaf area–length allometry and its implications in leaf shape evolution. *Trees* **33**, 1073-1085 (2019).

119 Ellis, R. P. A procedure for standardizing comparative leaf anatomy in the *Poaceae*. I. The leaf blade as viewed in transverse section. *Bothalia* **12**, 65-109 (1976).

120 Evert, R. F. *Esau's plant anatomy: meristems, cells, and tissues of the plant body: their structure, function, and development*. (John Wiley & Songs, 2006).

121 Neufeld, H. S. et al. Genotypic variability in vulnerability of leaf xylem to cavitation in water-stressed and well-irrigated sugarcane. *Plant Physiol.* **100**, 1020-1028 (1992).

122 Tyree, M. T., Zimmermann, M. H. & Zimmermann, M. H. *Xylem structure and the ascent of sap*. 2nd edn, (Springer, 2002).

123 Wright, I. J. et al. The world-wide leaf economics spectrum. *Nature* **428**, 821-827 (2004).

124 Aliscioni, S. et al. New grass phylogeny resolves deep evolutionary relationships and discovers C_4 origins. *New Phytol.* **193**, 304-312 (2012).

125 Taylor, S. H. et al. Photosynthetic pathway and ecological adaptation explain stomatal trait diversity amongst grasses. *New Phytol.* **193**, 387-396 (2012).

126 Edgar, R. C. MUSCLE: multiple sequence alignment with high accuracy and high throughput. *Nucleic Acids Res* **32**, 1792-1797 (2004).

127 Drummond, A. J. & Rambaut, A. BEAST: Bayesian evolutionary analysis by sampling trees. *Bmc Evol Biol* **7** (2007).

128 Christin, P. A. *et al.* Molecular Dating, Evolutionary Rates, and the Age of the Grasses. *Syst Biol* **63**, 153-165 (2013).

129 Prasad, V. et al. Late Cretaceous origin of the rice tribe provides evidence for early diversification in Poaceae. *Nat. Commun.* **2** (2011).

130 R: A language and environment for statistical computing (R Foundation for Statistical Computing, Vienna, Austria, 2019).

131 Paradis, E. & Schliep, K. ape 5.0: an environment for modern phylogenetics and evolutionary analyses in R. *Bioinformatics* **35**, 526-528(2019).

132 Spriggs, E. L., Christin, P. A. & Edwards, E. J. (ed Dryad Digital Repository) (2014).

133 Felsenstein, J. Phylogenies and the comparative method. *Am. Nat.* **125**, 1-15 (1985).

134 Schmerler, S. B. et al. Evolution of leaf form correlates with tropical–temperate transitions in Viburnum (Adoxaceae). *P. Royal. Soc. B.* **279**, 3905-3913 (2012).

135 Fletcher, L. R. et al. Evolution of leaf structure and drought tolerance in species of Californian Ceanothus. *Am. J. Bot.* **105**, 1672-1687 (2018).

136 Bramer, I. et al. in *Next Generation Biomonitoring: Part 1*: *Advances in Ecological Research* 101-161 (2018).

137 Zanne, A. E. et al. Three keys to the radiation of angiosperms into freezing environments. *Nature* **514**, 394-394 (2014).

138 Watcharamongkol, T., Christin, P. A. & Osborne, C. P. C_4 photosynthesis evolved in warm climates but promoted migration to cooler ones. *Ecol. Lett.* **21**, 376-383 (2018).

139 Burnham, K. P. & Anderson, D. R. *Model selection and multimodel inference*. 2 edn, (Springer, 2002).

140 Gelman, A. & Hill, J. *Data analysis using regression and multilevel/hierarchical models.* (Cambridge University Press, 2006).
141 Faraway, J. J. *Linear Models with R.* (Chapman & Hall/CRC, 2009).
142 Murray, K. & Conner, M. M. Methods to quantify variable importance: implications for the analysis of noisy ecological data. *Ecology* **90**, 348-355 (2009).
143 Westoby, M. & Wright, I. J. Land-plant ecology on the basis of functional traits. *Trends Ecol. Evol.* **21**, 261-268 (2006).
144 Grubb, P. J. Trade-offs in interspecific comparisons in plant ecology and how plants overcome proposed constraints. *Plant Ecol. Divers.* **9**, 3-33 (2016).
145 Cade, B. S. & Noon, B. R. A gentle introduction to quantile regression for ecologists. *Front. Ecol. Environ.* **1**, 412-420 (2003).
146 Grubb, P. J., Coomes, D. A. & Metcalfe, D. J. Comment on "A Brief History of Seed Size". *Science* **310**, 781-783 (2005).
147 Moles, A. T. *et al.* Global patterns in plant height. *J. Ecol.* **97**, 923-932 (2009).
148 Pagel, M. Inferring the historical patterns of biological evolution. *Nature* **401**, 877-884 (1999).
149 Freckleton, R. P., Harvey, P. H. & Pagel, M. Phylogenetic analysis and comparative data: A test and review of evidence. *Am. Nat.* **160**, 712-726 (2002).
150 “nlme” (R package version 3.1-140) (2019).
151 Revell, L. J. phytools: an R package for phylogenetic comparative biology (and other things). *Methods Ecol. Evol.* **3**, 217-223 (2012).
152 Warton, D. I., Wright, I. J., Falster, D. S. & Westoby, M. Bivariate line-fitting methods for allometry. *Biol. Rev.* **81**, 259-291 (2006).
153 Garland, T., Dickerman, A. W., Janis, C. M. & Jones, J. A. Phylogenetic Analysis of Covariance by Computer-Simulation. *Syst. Biol.* **42**, 265-292 (1993).
154 “nortest: Tests for normality” (R package version 1.0-4) (2015).
155 Poorter, H. & Sack, L. Pitfalls and possibilities in the analysis of biomass allocation patterns in plants. *Front. Plant Sci.* **3**, 1-10 (2012).
156 Smith, R. J. Use and Misuse of the Reduced Major Axis for Line-Fitting. *Am. J. Phys. Anthropol.* **140**, 476-486 (2009).
157 Gates, D. M. Energy, Plants, and Ecology. *Ecology* **46**, 1-13 (1965).

158 Lusk, C. H. et al. Frost and leaf-size gradients in forests: global patterns and experimental evidence. *New Phytol.* **219**, 565-573 (2018).

159 Muir, C. D. tealeaves: an R package for modelling leaf temperature using energy budgets. *Aob Plants* **11**, 1-10 (2019).

160 Taylor, S. H. et al. Ecophysiological traits in C_3 and C_4 grasses: a phylogenetically controlled screening experiment. *New Phytol.* **185**, 780-791 (2010).

161 Huang, M. et al. Air temperature optima of vegetation productivity across global biomes. *Nat. Ecol. Evol.* **3**, 772-779 (2019).

162 Farquhar, G. D., Caemmerer, S. V. & Berry, J. A. A biochemical model of photosynthetic CO_2 assimilation in leaves of C_3 species. *Planta* **149**, 78-90 (1980).

163 Bernacchi, C. J., Pimentel, C. & Long, S. P. In vivo temperature response functions of parameters required to model RuBP-limited photosynthesis. *Plant Cell Environ.* **26**, 1419-1430 (2003).

164 Muir, C. D. Making pore choices: repeated regime shifts in stomatal ratio. *P. Royal. Soc. B.* **282**, 1-9 (2012).

165 Brummitt, R. K. World geographical scheme for recording plant distributions. (2001).

166 Redmann, R. E. Adaptation of grasses to water-stress - leaf rolling and stomate distribution. *Ann. Mo. Bot. Gard.* **72**, 833-842 (1985).

167 Forrestel, E. J. et al. Different clades and traits yield similar grassland functional responses. *P. Natl. Acad. Sci. USA* **114**, 705-710 (2017).

168 Liu, H., Edwards, E. J., Freckleton, R. P. & Osborne, C. P. Phylogenetic niche conservatism in C_4 grasses. *Oecologia* **170**, 835-845 (2012).

169 Liu, H. & Osborne, C. P. Water relations traits of C_4 grasses depend on phylogenetic lineage, photosynthetic pathway, and habitat water availability. *J. Exp. Bot.* **66**, 761-773 (2015).

170 Jardine, E. C., Thomas, G. H., Forrestel, E. J., Lehmann, C. E. R. & Osborne, C. P. The global distribution of grass functional traits within grassy biomes. *J. Biogeogr.* **47**, 553-565 (2020).

171 Kawai, K. & Okada, N. Leaf vascular architecture in temperate dicotyledons: correlations and link to functional traits. *Planta* **251**, 1-12 (2019).

172 Medeiros, C. D. et al. An extensive suite of functional traits distinguishes Hawaiian wet and dry forests and enables prediction of species vital rates. *Funct. Ecol.* **33**, 712-734 (2019).

173 Li, F. L. et al. Linking leaf hydraulic properties, photosynthetic rates, and leaf lifespan in xerophytic species: a test of global hypotheses. *Am. J. Bot.* **105**, 1858-1868 (2018).

174 Blackman, C. J. et al. The links between leaf hydraulic vulnerability to drought and key aspects of leaf venation and xylem anatomy among 26 Australian woody angiosperms from contrasting climates. *Ann. Bot-London* **122**, 59-67 (2018).

175 Gleason, S. M. et al. Vessel scaling in evergreen angiosperm leaves conforms with Murray's law and area-filling assumptions: implications for plant size, leaf size and cold tolerance. *New Phytol.* **218**, 1360-1370 (2018).

176 Savi, T. et al. Morpho-anatomical and physiological traits in saplings of drought-tolerant Mediterranean woody species. *Trees-Struct. Funct.* **31**, 1137-1148 (2017).

177 Brodribb, T. J., Bienaime, D. & Marmottant, P. Revealing catastrophic failure of leaf networks under stress. *P. Natl. Acad. Sci. USA* **113**, 4865-4869 (2016).

178 Schneider, J. V. et al. Water supply and demand remain coordinated during breakdown of the global scaling relationship between leaf size and major vein density. *New Phytol.*. **214**, 473-486 (2017).

179 Coomes, D. A., Heathcote, S., Godfrey, E. R., Shepherd, J. J. & Sack, L. Scaling of xylem vessels and veins within the leaves of oak species. *Biol. Letters* **4**, 302-306 (2008).

180 Yao, G. Q. et al. Combined high leaf hydraulic safety and efficiency provides drought tolerance in Caragana species adapted to low mean annual precipitation. *New Phytol.* (2020).

181 McKown, A. D., Akamine, M. E. & Sack, L. Trait convergence and diversification arising from a complex evolutionary history in Hawaiian species of *Scaevola*. *Oecologia* **181**, 1083-1100 (2016).

182 Kawai, K. & Okada, N. How are leaf mechanical properties and water-use traits coordinated by vein traits? A case study in Fagaceae. *Funct. Ecol.* **30**, 527-536 (2016).

183 Dunbar-Co, S., Sporck, Margaret J. & Sack, L. Leaf Trait diversification and design in seven rare taxa of the hawaiian plantago radiation. *Int. J. Plant Sci.* **170**, 61-75 (2009).

184 Scoffoni, C. et al. Light-induced plasticity in leaf hydraulics, venation, anatomy, and gas exchange in ecologically diverse Hawaiian lobeliads. *New Phytol.*. **207**, 43-58 (2015).

185 Lu, Z. et al. Potassium mediates coordination of leaf photosynthesis and hydraulic conductance by modifications of leaf anatomy. *Plant Cell Environ.* **42**, 2231-2244 (2019).

186 Nardini, A., Peda, G. & La Rocca, N. Trade-offs between leaf hydraulic capacity and drought vulnerability: morpho-anatomical bases, carbon costs and ecological consequences. *New Phytol.* **196**, 788-798 (2012).

187 Brocious, C. A. & Hacke, U. G. Stomatal conductance scales with petiole xylem traits in Populus genotypes. *Funct. Plant Biol.* **43**, 553-562 (2016).

188 Mauri, R. et al. Leaf hydraulic properties are decoupled from leaf area across coffee species. *Trees* **34**, 1507-1514 (2020).

189 Nardini, A., Ounapuu-Pikas, E. & Savi, T. When smaller is better: leaf hydraulic conductance and drought vulnerability correlate to leaf size and venation density across four Coffea arabica genotypes. *Funct. Plant Biol.* **41**, 972-982 (2014).

190 Mediavilla, S., Martín, I. & Escudero, A. Vein and stomatal traits in leaves of three co-occurring Quercus species differing in leaf life span. *Eur. J. For. Res.* **139**, 829-840 (2020).

191 Wang, J.-H., Cai, Y.-F., Li, S.-F. & Zhang, S.-B. Photosynthetic acclimation of rhododendrons to light intensity in relation to leaf water-related traits. *Plant Ecol.* **221**, 407-420 (2020).

192 Cardoso, A. A. et al. Extended differentiation of veins and stomata is essential for the expansion of large leaves in *Rheum rhabarbarum*. *Am. J. Bot.* **105**, 1967-1974 (2018).

193 Taneda, H. & Terashima, I. Co-ordinated development of the leaf midrib xylem with the lamina in *Nicotiana tabacum*. *Ann. Bot.* **110**, 35-45 (2012).

194 Sevanto, S., Holbrook, N. M. & Ball, M. C. Freeze/Thaw-Induced embolism: probability of critical bubble formation depends on speed of ice formation. *Front. Plant Sci.* **3**, 1-12 (2012).

195 McKown, A. D., Cochard, H. & Sack, L. Decoding leaf hydraulics with a spatially explicit model: Principles of venation architecture and implications for its evolution. *Am. Nat.* **175**, 447-460 (2010).

196 Spriggs EL, Christin P-A, Edwards EJ (2014) C_4 Photosynthesis promoted species diversification during the miocene grassland expansion. *PloS One* **9**, 1-10 (2014).

Acknowledgments

We thank T Cheng, W Deng, A.C. Diener, A Kooner, M McMaster, C Muir, S Moshrefi, A. J. Patel, A Sayari and M. S. Vorontsova for logistical assistance. **Funding:** Funding was provided by the U.S. National Science Foundation (grants 1457279, 1951244 and 2017949), the Natural Environment Research Council (grants NE/DO13062/1 and NE/T000759/1) and a Royal Society University Research Fellowship (grant URF\R\180022).

Author contributions

Conceptualization: ASB, SHT, CPO, LS; *Data curation & Writing – review & editing*: ASB, SHT, JPK, CV, YZ, TW, CS, EJE, PAC, CPO, LS; *Formal analysis*: ASB, SHT, JPK, CV, YZ, TW, CS, PAC, LS; *Funding acquisition:* CPO, LS; *Investigation:* ASB, SHT, JPK, TW, CS, EJE, PAC, CPO, LS; *Methodology:* ASB, SHT, JPK, TW, CS, EJE, PAC, CPO, LS; *Project administration:* ASB, SHT, JPK, CPO, LS *Resources:* ASB, SHT, JPK, TW, CS, EJE, PAC, CPO, LS; *Software:* ASB, SHT, TW, PAC; *Supervision:* ASB, SHT, JPK, CPO, LS; *Validation:* ASB, SHT, CPO, LS; *Visualization:* ASB, SHT, TW, CV, PAC; *Writing – original draft:* ASB, SHT, LS

Competing interests

We declare no competing interests. All data are available in the main text or supplementary materials.

Additional information

Supplementary information is available online. Reprints and permissions information is available online at www.nature/com/reprints. Correspondence and requests for materials should be addressed to A.S.B.

Data availability

Data utilized in this study are provided in the supplementary materials. Leaf trait data for the 1752 grass species was provided by the published Kew Grassbase Database (http://www.kew.org/data/grassbase/). Species' climate data were extracted from WorldClim 2 5-arc minute resolution (https://worldclim.org/version2) and from CRU TS4.01 01 (https://crudata.uea.ac.uk/cru/data/hrg/cru_ts_4.01/) based on each species' geographical records (http://www.gbif.org). Photosynthetic trait data and field locations were extracted for the 13 C_3 grass species for which this was available in GLOPNET (http://bio.mq.edu.au/~iwright/glopian.htm).

Code availability

Custom-written R code is available on GitHub (https://github.com/smuel-tylor/grass-leaf-size-).

Extended Data Figure Legends

Extended Data Fig. 1 Time-calibrated phylogenetic trees for 1752 worldwide grass species and for 27 grass species grown in a greenhouse common garden. (a) phylogeny for 1752 species trimmed from that of reference 196 and used for analyses of global scaling of leaf size with climate. C_3 and C_4 species in black and red respectively (n = 840 and n = 912 respectively). **(b)** phylogeny for 27 species used for analyses of leaf vein scaling (black branches = 11 C_3, red branches = 16 C_4), emphasizing the inclusion of 11 independent C_4 origins. World map with distributions of **(c)** 11 C_3 species and, **(d)** 16 C_4 species.

Extended Data Fig. 2. Worldwide relationships of grass leaf and plant dimensions with species' native climate, the global distribution of grass leaf size, and the scaling of grass leaf and plant dimensions. Relationships of **(a) – (c)** Leaf length, **(d) – (f)** leaf width, **(g) – (i)** leaf area, and **(j) – (l)** culm height with mean annual temperature (MAT, °C), mean annual precipitation (MAP, mm) and aridity index (AI). **(m-o)** Average across species of leaf area for each country in the global database (International Working Group on Taxonomic Databases for Plant Sciences, TDWG level 3 spatial units[168]), including countries for which > 20 species occur in the global database (21 – 547 species for each country; gray for countries with < 20 species represented), i.e., **(m)** mean leaf area **(n)** median leaf area and **(o)** leaf area for the largest leafed species **(p)** The scaling of leaf area with leaf length and **(q)** leaf width, **(r)** leaf area with culm height, **(s)** culm height with leaf length and **(t)** leaf width and **(u)** leaf width with leaf length. Leaf trait and climate data provided in Supplementary Table 2. N = 1752 globally distributed grass species in panels **(a) – (i), (p), (q) and (u)** and 1729 in panels **(j) – (l), (r), (s)** and **(t)**. Corresponding regression coefficients for ahistorical analyses of relationships in panels **(a) – (l):** 0.14, 0.17, 0.14, 0.26, 0.34, 0.28, 0.24, 0.31, 0.26, 0.24, 0.29, and 0.3. Two-tailed phylogenetically reduced major axis (PRMA) regressions were fitted for log (trait) = log (a) + b log (trait) in panels **(a)** – **(l)** and **(p)** – **(u)**. Significance: ***$P < 0.001$, **$P < 0.01$. P = **(a)** 0.0099, **(b)** 7.8×10^{-9}, **(c)** 4.2×10^{-9}, **(d)** 0.004**, (e)** 1.8×10^{-8}, **(f)** 2.4×10^{-11}, **(g)** 0.0014**, (h)** 2.9×10^{-11}, **(i)** 2.2×10^{-13}, **(j)** 1.7×10^{-6}, **(k)** 4.0×10^{-7}, **(l)** 1.1×10^{-5}, **(p)** ~ 0 , **(q)** ~ 0 , **(r)** 3.17×10^{-219}, **(s)** 1.92×10^{-205}, **(t)** 7.92×10^{-106} and **(u)** 2.7×10^{-96}. C_3 and C_4 species in red and blue, respectively.

Extended Data Fig. 3. Worldwide association of grass leaf size with species' native climate in 3D, and binned by 1/3rd lowest, middle and highest mean annual temperature (MAT, °C), or mean annual precipitation (MAP, mm) in 2D. (a) Leaf area (cm^2) versus climate variables, i.e. x = mean annual temperature (MAT, °C) and y = mean annual precipitation (MAP, mm) in panel **(a)** and **(c)**, and the horizontal axes are flipped, i.e., leaf area versus x = MAP and y = MAT in panels **(b)** and **(d)**. Relationships of **(e) – (g)** Leaf length, **(h) – (j)** leaf width, **(k) – (m)** leaf area, and **(n)** – **(p)** culm height with mean annual precipitation (mm); n = 584 globally distributed grass species in panels **(e) – (m)** and 576 for panels **(n) – (p).** Relationships of **(q) – (s)** Leaf length, **(t) – (v)** leaf width, **(w) – (y)** leaf area, and **(z)** – **(bb)** culm height with mean annual temperature (°C). N = 584 globally distributed grass species in panels **(e) – (m) and (q) – (y)** and 576 for panels **(n) – (p) and (z) – (bb).** Panels **(a)** and **(b)** present the data for all species in the global database (N = 1752); panels **(c)** and **(d)** exclude the 29 species with MAT < 0 °C, for a clearer view of the bulk of the species. Projected grey shadows in **(a) – (d)** represent the bivariate relationships. Parameters from multiple regression analysis are presented in Supplementary Table 8. Two-tailed ordinary least square (OLS) regressions were fitted for log (trait) = log (a) + b log (climate variable) in panels **(e)** – **(bb)**. Significance: ***$P < 0.001$, **$P < 0.01$. P = **(e)** 8.1×10^{-5}, **(f)** 2.2×10^{-5}, **(g)** 0.0002, **(h)** 0.0094, **(i)** 8.4×10^{-28}, **(j)** 1.7×10^{-21}, **(k)**

0.0002, **(l)** 1.1 × 10^{-20}, **(m)** 1.8 × 10^{-15}, **(n)** 0.0028, **(o)** 4.7 × 10^{-25}, **(p)** 2.2 × 10^{-10}, **(q)** 0.0106, **(r)** 2.9 × 10^{-6}, **(t)** 7.0 × 10^{-5}, **(u)** 6.7 × 10^{-6}, **(v)** 1.5 × 10^{-17}, **(w)** 0.0001, **(x)** 7.9 × 10^{-8}, **(y)** 2.6 × 10^{-11}, **(z)** 1.3 × 10^{-5}, **(aa)** 1.7 × 10^{-9} and **(bb)** 8.5 × 10^{-10}**.** C_3 and C_4 species in red and blue, respectively.

Extended Data Fig. 4. Quantile regression analyses of worldwide associations of grass leaf traits with species' native climate. Relationships of **(a) – (c)** Leaf length, **(d) – (f)** leaf width, **(g) – (i)** leaf area, and **(j)** – **(l)** culm height with mean annual temperature (MAT, °C), mean annual precipitation (MAP, mm) and aridity index (AI). N = 1752 globally distributed grass species in panels **(a) – (i)** and 1729 in panels **(j) – (l).** Two-tailed ordinary least square (OLS; solid lines) and 95% and 5% quantile regressions (dotted lines) were fitted for log (trait) = log (a) + b log (climate variable); quantile lines drawn if significantly different in slope at $P < 0.05$. C_3 and C_4 species in red and blue respectively.

Extended Data Fig. 5. Worldwide associations of grass leaf and plant dimensions with species' native climate, for species with leaf width < 8.16 cm or < 4.47 cm, i.e. below the modelled threshold for damage due to night time chilling or overheating, and modeled leaf temperature difference from air temperature for amiphistomatous grass leaves under different air temperatures. Relationships of **(a) – (b)** Leaf length, **(c) – (d)** leaf width, **(e) – (f)** leaf area, and **(g) – (h)** culm height with mean annual temperature (MAT, °C) and mean annual precipitation (MAP, mm) for species with leaf width < 8.16 cm. Relationships of **(i) – (j)** Leaf length, **(k) – (l)** leaf width, **(m) – (n)** leaf area, and **(o) – (p)** culm height with mean annual temperature (MAT, °C) and mean annual precipitation (MAP, mm) for species with leaf width < 4.47 cm. N = 1748 globally distributed grass species for panels **(a) – (f)**, 1725 for panels **(g) – (h)**, 1716 for panels **(i) – (n)** and 1694 for panels **(o) – (p).** Simulations were run with stomatal conductance (mol m^{-2} s^{-1}) **(q) – (t)** 0.1, **(u) – (x)** 0.2 and **(y) – (bb)** 0.4, and wind speed (m/s), at **(q), (u) and (y)** 0.1, **(r), (v) and (z)** 0.5, **(s), (w) and (aa)** 1, **(t), (x) and (bb)** 2, with leaf width (cm) of 0.04, 0.1, 0.5, 0.9, 1.5, 2.7 and 11 shown as increasing darker blue lines. No difference in leaf temperature from air temperature line in red. Two-tailed ordinary least square (OLS) regressions were fitted for log (trait) = log (a) + b log (climate variable) in panels **(a)** – **(p)**. Significance: ***$P < 0.001$, **$P < 0.01$, *$P < 0.05$. P = **(a)** 2.1 × 10^{-8}, **(b)** 6.2 × 10^{-13}, **(c)** 4.7 ×

10^{-29} , **(d)** 6.2×10^{-48} , **(e)** 2.0×10^{-24}**, (f)** 6.8×10^{-40}, **(g)** 1.9×10^{-24}, **(h)** 1.3×10^{-33}, **(i)** 2.4×10^{-7}, **(j)** 7.4×10^{-11}, **(k)** 1.0×10^{-26}, **(l)** 3.4×10^{-39}, **(m)** 5.4×10^{-22}, **(n)** 9.8×10^{-33}, **(o)** 4.4×10^{-22} and **(p)** 3.8×10^{-29}. C_3 and C_4 species in red and blue respectively.

Extended Data Fig. 6. Worldwide scaling of grass vein length per leaf area and vein diameter with leaf size and species' native climatic aridity, and of vein xylem conduit diameter with vein diameter. Relationships of major vein length per area with **(a)** and **(c)** leaf width, **(b)** and **(d)** leaf area and **(c)** aridity index (AI) (where lower values correspond to greater climatic aridity). Relationships of vein diameters with **(f, i, l, o)** leaf length, (**g, j, m, p**) leaf width and **(h, k, n, q**) leaf area (= leaf length × leaf width). Relationships of vein length per area with **(r, u, x, aa)** leaf length, **(s, v, y, bb)** leaf width and **(t, w, z, cc)** leaf area (leaf length × leaf width). Relationships of vein xylem conduit diameters with vein diameter **(dd)** first order (1°) veins**, (ee)** second order (2°) veins**, (ff)** third order (3°) veins and **(gg)** fourth order (4°)**.** $N = 616$ species in panels **(a),** 600 in panel **(b)**, 170 in panel **(c),** 166 in panel **(d)**, 21 in panel **(e)**, 27 in panels **(f)** – **(ff)** and 7 in panel **(gg)**. Two-tailed ordinary least square (OLS) regressions, phylogenetic generalized least square (PGLS) or phylogenetic reduced major axis (PRMA) regressions were fitted for log (trait) = log (a) + b log (trait or climate variable) in panels **(a)** and **(b)**, **(c)** and **(d)**, and **(e)**, respectively. Phylogenetic reduced major axis (PRMA) or phylogenetic generalized least square (PGLS) regressions were fitted for log (vein diameter or vein length per area) = log (a) + b log (leaf length, width, or leaf area) in panels **(f)** – **(q)**, and **(r)** – **(cc)**, respectively. Phylogenetic reduced major axis (PRMA) regressions were fitted for log (xylem conduit diameter) = log (a) + b log (vein diameter) in panels **(dd)** – **(gg)**. $P^* < 0.05$, $P^{**} < 0.01$, $P^{***} < 0.001$. P = **(a)** 9.4×10^{-250}, **(b)** 1.6×10^{-139} , **(c)** 7.0×10^{-46}, **(d)** 1.0×10^{-31}, **(e)** 0.0051**, (f)** 0.0007, **(h)** 3.0×10^{-5}, **(i)** 3.9×10^{-6} , **(k)** 0.0003, **(s)** 1.2×10^{-34}, **(t)** 7.0×10^{-04}, **(v)** 1.4×10^{-7}, **(w)** 0.0167, **(bb)** 0.0020, **(dd)** 0.0110 and **(ee)** 0.0004. Line parameters for panels **(f)** – **(cc)** in Table 1 and Supplementary Table 10 and for **(dd)** – **(gg)** in Supplementary Table 11. Significant relationships are plotted with PRMA to illustrate the central trends (see *Methods*). C_3 and C_4 species in white and grey respectively. Standard errors for species trait values are found in Supplementary Table 3.

Extended Data Fig. 7. Scaling of leaf vein projected area, vein surface area and vein volume of given vein orders with leaf dimensions across 27 C_3 and C_4 grass species grown experimentally. Relationships of vein projected area with **(a, d, g, j)** leaf length, **(b, e, h, k)** leaf width and **(c, f, i, l)** leaf area (leaf width × leaf length). Relationships of vein surface area with **(m, p, s, v)** leaf length, **(n, q, t, w)** leaf width, and **(o, r, u, x)** leaf area (leaf length × leaf width). Relationships of vein volume with **(y, bb, ee, hh)** leaf length, (z, cc, ff, ii) leaf width, and (aa, dd, gg, jj) leaf area (leaf width × leaf length). Two-tailed phylogenetic generalized least square (PGLS) regressions were fitted for log (vein projected area, vein surface area per area or vein volume) = log (a) + b log (leaf length, width, or area) and drawn when significant. $P^* < 0.05$, $P^{**} < 0.01$, $P^{***} < 0.001$; line parameters in Supplementary Table 10. P = **(a)** 0.0011, **(b)** 1.2×10^{-12}, **(d)** 0.0011**, (e)** 7.0×10^{-5}**, (g)** 0.0335, **(h)** 0.0161**, (k)** 0.0167**, (m)** 0.0011**, (n)** 1.2×10^{-12} **,** **(p)** 0.0011**, (q)** 7.0×10^{-5}, **(s)** 0.0335, **(t)** 0.0161, **(w)** 0.0167, **(y)** 8.2×10^{-6}, **(z)** 5.4×10^{-6}, **(bb)** 5.2×10^{-5}, **(cc)** 0.0037 and **(ff)** 0.0093**.** Significant trends are plotted with PRMA to illustrate the central trends (see methods). Standard errors for species trait values are found in Supplementary Table 3. C_3 and C_4 species in white and grey respectively.

Extended Data Fig. 8. Partitioning of the contributions of given vein orders of the venation architecture of C_3 and C_4 grasses, with minor veins accounting for the differences in vein length per area. **(a)** *Triticum aestivum*, a C_3 species. **(b)** *Aristida ternipes*, a C_4 species without 4° veins ($C_{4\text{-}3L}$; i.e., third-order veins are the highest longitudinal vein order). **(c)** *Paspalum dilatum,* a C_4 species with 4° veins ($C_{4\text{-}4L;}$ i.e., fourth-order veins are the highest longitudinal vein order). **(d)** Vein length per area (cm cm^{-2}) distribution across vein orders for each type (C_3 n = 11, C_4-3L = 9, C_4-4L = 7). **(e)** Vein length per unit area, **(f)** vein surface area per unit leaf area, **(g)** vein projected area per unit leaf area and **(h)** vein volume per unit leaf area distribution across vein orders for each type (C_3 n = 11, C_4 = 16). Statistical comparisons by phylogenetic ANOVA are presented in Supplementary Table 3.

Extended Data Fig. 9. Associations of light-saturated leaf photosynthetic rate with native climate and vein traits for terrestrial C_3 species, and the scaling of transverse 5° vein length per area (5° VLA) with major vein length per area (major VLA) across 27 C_3 and C_4 grass species grown experimentally. Relationships of area-based light-saturated photosynthetic rate

(A_{area}), measured with photosynthesis systems, with (a) mean annual temperature (MAT, °C), (b) mean annual precipitation (MAP, mm), and (c) and growing season length (GSL, month). Relationships of light-saturated photosynthetic rate per area with (d) major vein length per area (VLA_{major}, cm cm^{-2}) and (e) major vein surface area per area (VSA_{major}, unitless), and (f) (transverse vein length per area ($VLA_{transverse}$, cm cm^{-2}) with VLA_{major}. Points and lines in red represent 8 terrestrial C_3 grasses of this study grown in a greenhouse common garden, related to the mean climate of their native distribution, supporting the assumption of higher photosynthetic rate in colder and drier climates with shorter growing seasons. Open points represent 13 Northern Hemisphere temperate terrestrial C_3 grass species from the global plant trait network (GLOPNET; ref 126) measured in the field, as related to the mean climate at their field site. Black lines represent the significant trend through all the points in panels **(a)** and **(c)**, which, given the disparate data sources combined here (and the consideration of field site rather than native range climate for the GLOPNET species), provides yet stronger support for the generality of the relationships of A_{area} to MAT and GSL. Notably, these are conservative tests of the relationships of photosynthetic rate with native climate, as measurements of A_{area} using the photosynthesis system chamber do not include the effect of the boundary layer conductance, which is made very high and invariant[23]. Under natural conditions, and especially under slow windspeeds, smaller leaves would have higher boundary layer conductances than larger leaves (see simulation in Extended Data Fig. 5), and thus, under natural conditions, including the effects of boundary layer, a yet stronger trend would be expected for small-leaved species of colder and drier climates to have higher photosynthetic rates than larger-leaved species of warm, moist climates. Two-tailed ordinary least square (OLS) regressions or phylogenetic reduced major axis (PRMA) were fitted for log (trait) = log (a) + b log (trait or climate variable) in panels **(a)** – **(e)** and **(f)**, respectively. Significance: $P* < 0.05$, $P** < 0.01$, $P^{x} = 0.04$ in a one-tailed test of the hypothesized positive correlation. P = **(a)** 0.0301 red line; 0.0071 black line, **(b)** 0.0183, **(c)** 0.0474 red line; 0.0021 black line, **(d)** 0.0794, **(e)** 0.0138 and **(f)** 0.0061**.** Error bars represent standard errors in panels **(a)** – **(e)**. Standard errors for species trait values in panel **(f)** are found in Supplementary Table 3. C_3 and C_4 species in white and grey, respectively, in panel **(e)**.

Extended Data Fig. 10. Estimating leaf size from venation traits that can be measured on small samples or fragments of grass leaves. (a) Leaf area and **(b)** leaf width predicted from 2°

vein length per area. N = 600 and 616 in panels **(a)** and **(b)** respectively (Grassbase dataset; Supplementary Table 2). The relationships were fitted with two-tailed ordinary least square (OLS) regressions. These relationships would enable the determination of intact leaf size from fragments that include at least two 2° veins, including fragmentary fossil remains. The 95% confidence intervals are in blue and 95% prediction intervals in red. $P^{***} < 0.001$. P = **(a)** 1.4×10^{-127} and **(b)** 7.6×10^{-227}.

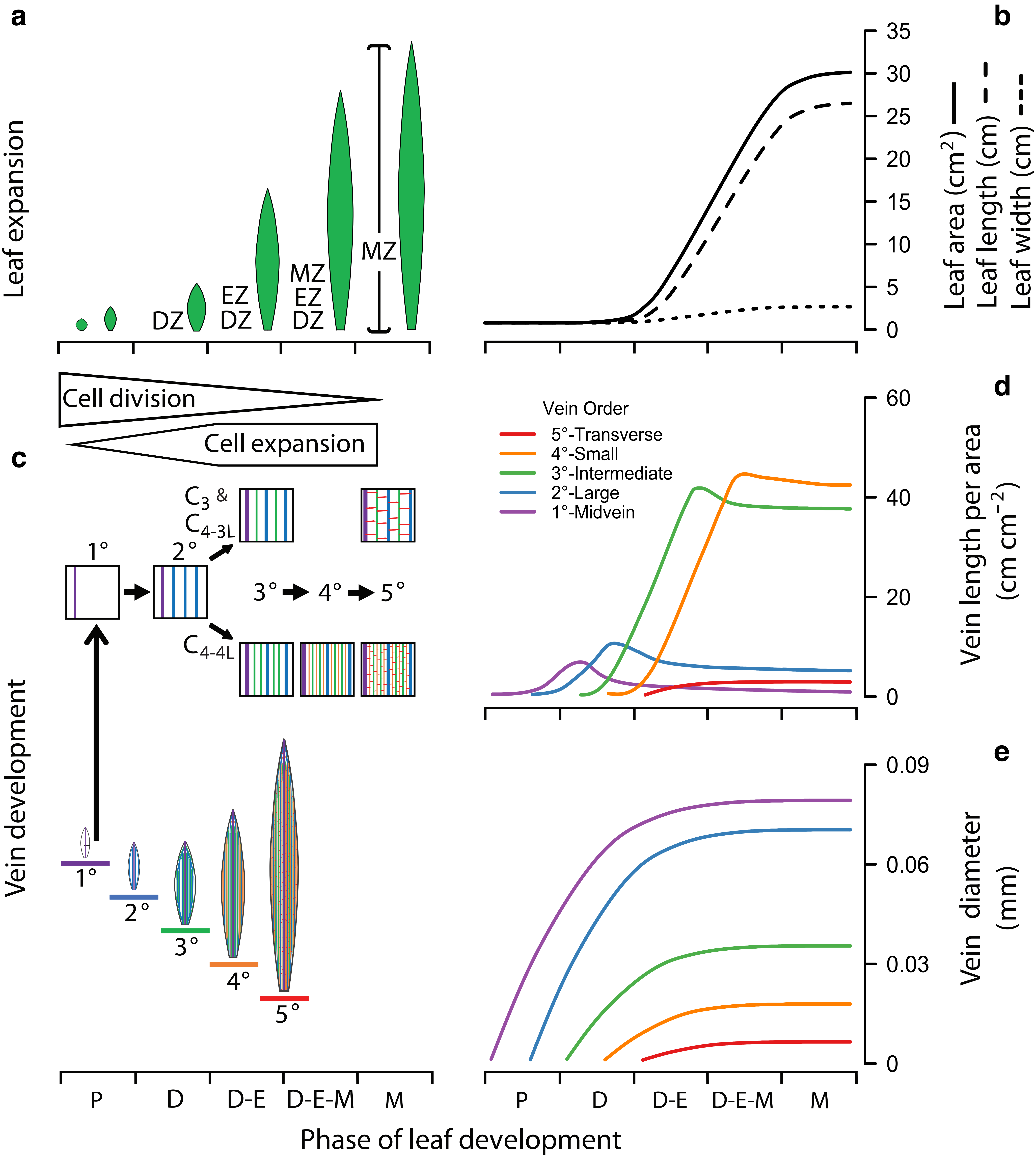
a
b
c
d
e
Leaf expansion
DZ
EZ
DZ
MZ
EZ
DZ
MZ
Leaf area (cm^2)
Leaf length (cm)
Leaf width (cm)
Cell division
Cell expansion
C_3 &
$C_{4\text{-}3L}$
$C_{4\text{-}4L}$
1°
2°
3° → 4° → 5°
Vein Order
5°-Transverse
4°-Small
3°-Intermediate
2°-Large
1°-Midvein
Vein length per area (cm cm^{-2})
Vein diameter (mm)
Vein development
P
D
D-E
D-E-M
M
Phase of leaf development

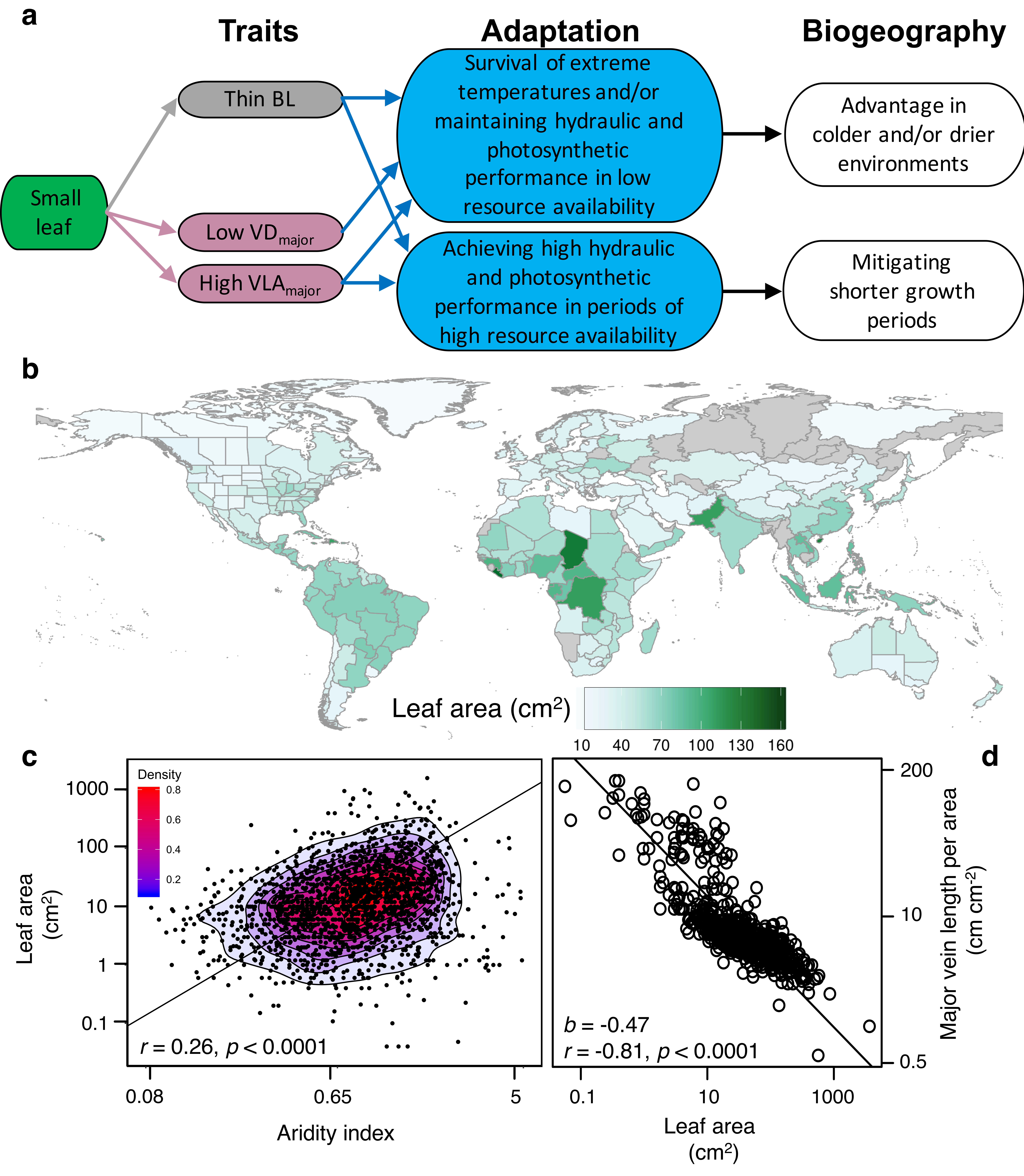

a
Traits
Adaptation
Biogeography
Small leaf
Thin BL
Low VD$_{major}$
High VLA$_{major}$
Survival of extreme temperatures and/or maintaining hydraulic and photosynthetic performance in low resource availability
Achieving high hydraulic and photosynthetic performance in periods of high resource availability
Advantage in colder and/or drier environments
Mitigating shorter growth periods
b
Leaf area (cm^2)
10 40 70 100 130 160
c
Density
0.8
0.6
0.4
0.2
1000
100
10
1
0.1
Leaf area (cm^2)
r = 0.26, p < 0.0001
0.08
0.65
5
Aridity index
d
200
10
0.5
Major vein length per area (cm cm^{-2})
b = -0.47
r = -0.81, p < 0.0001
0.1
10
1000
Leaf area (cm^2)

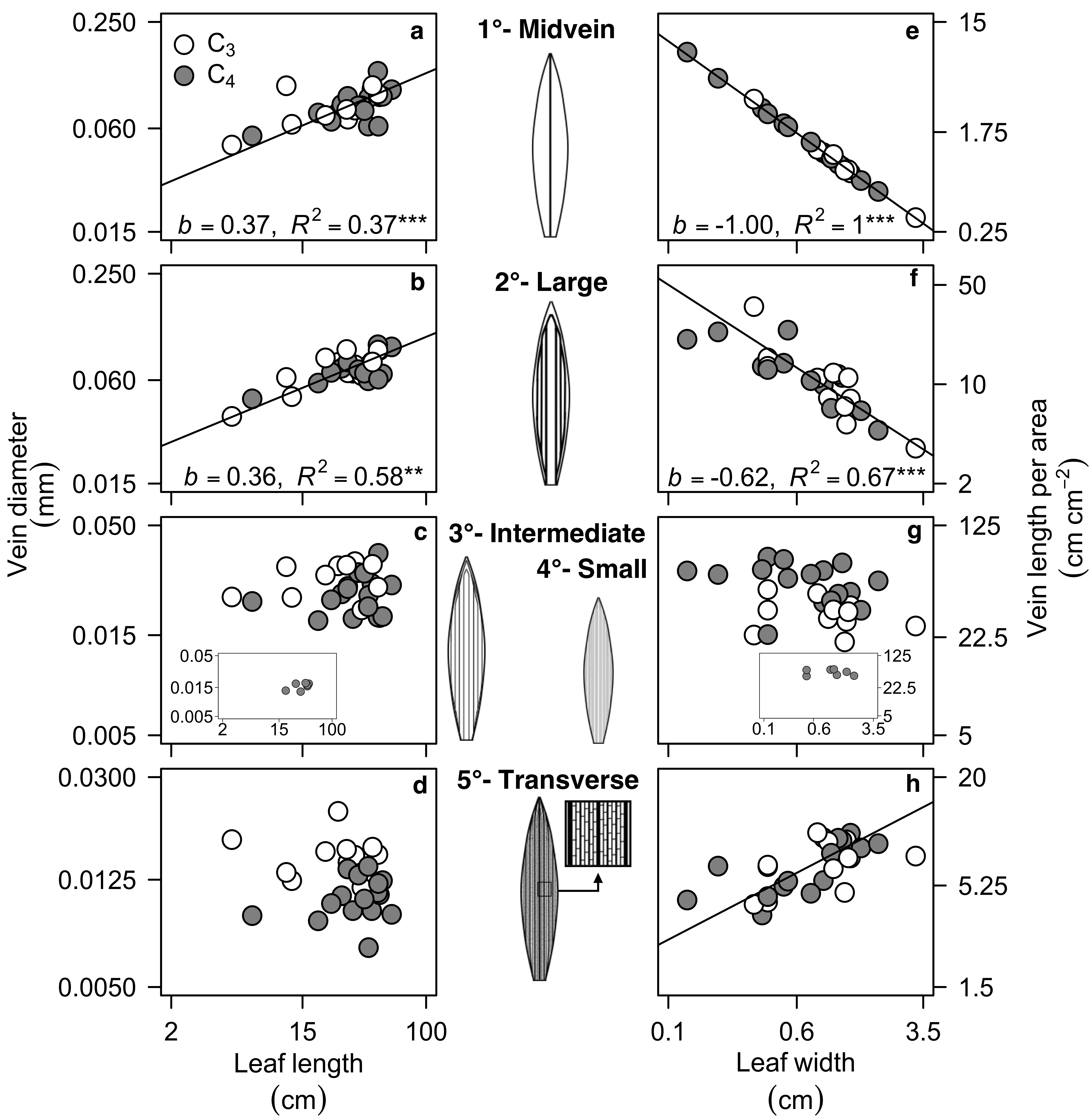

1°- Midvein
2°- Large
3°- Intermediate
4°- Small
5°- Transverse
a
b
c
d
e
f
g
h
C3
C4
b = 0.37, R2 = 0.37***
b = 0.36, R2 = 0.58**
b = -1.00, R2 = 1***
b = -0.62, R2 = 0.67***
Vein diameter (mm)
Vein length per area (cm cm−2)
Leaf length (cm)
Leaf width (cm)
0.250
0.060
0.015
0.050
0.005
0.0300
0.0125
0.0050
0.05
2
15
100
15
1.75
0.25
50
10
125
22.5
5
20
5.25
1.5
0.1
0.6
3.5